

Learning Latent Features with Pairwise Penalties in Matrix Completion

Kaiyi Ji*, Jian Tan†, Yuejie Chi‡ and Jinfeng Xu§

February 15, 2018

Abstract

Low-rank matrix completion (MC) has achieved great success in many real-world data applications. A latent feature model formulation is usually employed and, to improve prediction performance, the similarities between latent variables can be exploited by pairwise learning, e.g., the graph regularized matrix factorization (GRMF) method. However, existing GRMF approaches often use a squared L_2 norm to measure the pairwise difference, which may be overly influenced by dissimilar pairs and lead to inferior prediction. To fully empower pairwise learning for matrix completion, we propose a general optimization framework that allows a rich class of (non-)convex pairwise penalty functions. A new and efficient algorithm is further developed to uniformly solve the optimization problem, with a theoretical convergence guarantee. In an important situation where the latent variables form a small number of subgroups, its statistical guarantee is also fully characterized. In particular, we theoretically characterize the complexity-regularized maximum likelihood estimator, as a special case of our framework. It has a better error bound when compared to the standard trace-norm regularized matrix completion. We conduct extensive experiments on both synthetic and real datasets to demonstrate the superior performance of this general framework.

1 Introduction

Low-rank matrix factorization (MF) has been widely used in many real-world data applications, e.g., in signal processing, image restoration and collaborative filtering. A typical optimization problem (Koren et al., 2009; Gopalan et al., 2014) follows the form

$$\min_{\mathbf{X}, \mathbf{Y}} \frac{1}{2} \|\Psi_{\Omega}(\mathbf{M} - \mathbf{X}\mathbf{Y}^T)\|_F^2 + \frac{\alpha}{2} (\|\mathbf{X}\|_F^2 + \|\mathbf{Y}\|_F^2) \quad (1)$$

where $\mathbf{M} \in \mathbb{R}^{n \times m}$, $\mathbf{X} \in \mathbb{R}^{n \times d}$, $\mathbf{Y} \in \mathbb{R}^{m \times d}$ and the projection operator $\Psi_{\Omega}(\mathbf{M})$ retains the entries of the matrix \mathbf{M} in Ω that denotes the observed indices.

The row vectors $\{\mathbf{x}_i\}$ of \mathbf{X} and $\{\mathbf{y}_j\}$ of \mathbf{Y} usually represent the features of two classes of interdependent objects, known as latent variables, e.g., user features and movie features in recommender systems (Bennett

*Department of Electrical and Computer Engineering, The Ohio State University; e-mail: ji.367@osu.edu

†Department of Electrical and Computer Engineering, The Ohio State University; e-mail: tan.252@osu.edu

‡Department of Electrical and Computer Engineering, Carnegie Mellon University; e-mail: yuejiechi@cmu.edu

§Department of Statistics and Actuarial Science, The University of Hong Kong; e-mail: xujf@hku.hk

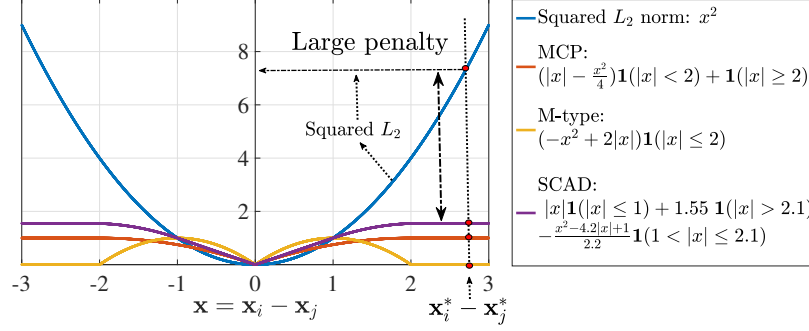


Figure 1: Illustration of three pairwise penalty functions w.r.t. $x = x_i - x_j$. When $x^* = x_i^* - x_j^*$ is large, the squared L_2 norm is much larger than MCP, SCAD and the M-type function.

et al., 2007; Koren et al., 2009), respectively. Based on this basic model, many variants have been considered for different application scenarios. For example, a latent feature model is often employed in matrix completion and, for a better estimation error, the similarities between latent variables can be exploited by pairwise learning, e.g. the graph regularized matrix factorization (GRMF) method using a squared L_2 norm. It has been shown that GRMF can reduce the recovery error (Rao et al., 2015; Zhao et al., 2015; Monti et al., 2017). For the ground truth $\mathbf{M}^* = \mathbf{X}^* \mathbf{Y}^{*T}$, assume that the feature vectors $\{\mathbf{x}_i^*\}$ correspond to the vertices of a graph (V^x, E^x, \mathbf{W}) with $V^x = \{1, 2, \dots, n\}$ and the edges $E^x = V^x \times V^x$ are weighted by a non-negative matrix $\mathbf{W} = [w_{ij}] \in \mathbb{R}^{n \times n}$. Similarly, we can also define (V^y, E^y, \mathbf{U}) for $\{\mathbf{y}_j^*\}$. By adding a smoothing graph regularizer to (1), GRMF aims to solve the problem

$$\begin{aligned} \min_{\mathbf{X}, \mathbf{Y}} \frac{1}{2} \|\Psi_{\Omega}(\mathbf{M} - \mathbf{X}\mathbf{Y}^T)\|_F^2 + \frac{\alpha}{2} (\|\mathbf{X}\|_F^2 + \|\mathbf{Y}\|_F^2) \\ + \gamma_X \sum_{i < j} w_{ij} \|\mathbf{x}_i - \mathbf{x}_j\|_2^2 + \gamma_Y \sum_{s < t} u_{st} \|\mathbf{y}_s - \mathbf{y}_t\|_2^2, \end{aligned} \quad (2)$$

which encourages the solutions $\mathbf{x}_i \approx \mathbf{x}_j$ (respectively $\mathbf{y}_s \approx \mathbf{y}_t$) if the weight w_{ij} (respectively u_{st}) is large.

Existing works (Ma et al., 2011a; Kalofolias et al., 2014; Rao et al., 2015; Zhao et al., 2015) often construct the weight matrices \mathbf{W} and \mathbf{U} by incorporating additional information of the feature vectors, e.g., the social network of users and the attributes of movies in recommender systems. However, as shown in (Chiang et al., 2015), the side information could have noise, and hence the weights may be inappropriately selected. As illustrated in Fig. 1, if the difference between \mathbf{x}_i^* and \mathbf{x}_j^* is large but w_{ij} is not small enough, the squared L_2 norm used in the graph regularizer can severely penalize the objective function and push the solution \mathbf{x}_i to be close to \mathbf{x}_j . It can result in biased estimates, as shown in (Ma & Huang, 2017), which can dramatically affect the recovery performance. The same argument also applies to \mathbf{y}_s and \mathbf{y}_t . To address this problem, we introduce a large family of (non-)convex pairwise penalty functions that imposes less penalization on large differences, e.g., by the minimax concave penalty (MCP) (Zhang, 2010), the smoothly clipped absolute deviation (SCAD) (Fan & Li, 2001), and the M-type function, as shown in Fig. 1. To this end, we propose a general optimization framework

$$\begin{aligned} \min_{\mathbf{X}, \mathbf{Y}} \frac{1}{2} \|\Psi_{\Omega}(\mathbf{M} - \mathbf{X}\mathbf{Y}^T)\|_F^2 + \frac{\alpha}{2} (\|\mathbf{X}\|_F^2 + \|\mathbf{Y}\|_F^2) \\ + \sum_{i < j} w_{ij} p(\mathbf{x}_i - \mathbf{x}_j, \gamma_X) + \sum_{s < t} u_{st} p(\mathbf{y}_s - \mathbf{y}_t, \gamma_Y), \end{aligned} \quad (3)$$

where $p(\cdot, \gamma_X)$ and $p(\cdot, \gamma_Y)$ are (non-)convex pairwise penalty functions with tuning parameters $\gamma_X, \gamma_Y \geq 0$.

To efficiently solve the whole class of optimization problems, we design a *novel and scalable* algorithm based on a modified alternating direction method of multipliers (ADMM) (Boyd et al., 2011). The allowed non-convex and non-smooth pairwise penalty functions complicate the optimization, which, if not handled carefully, can even result in divergent iterations. Theoretically, we characterize the convergence of our algorithm for the whole class of pairwise penalty functions. Compared with the standard ADMM, our algorithm has the following two features. First, although recent works (Wang et al., 2015a; Hong et al., 2016; Wang et al., 2015b) prove the convergence of ADMM for a large family of non-convex functions under different conditions, none of these results directly apply to our problem. Thus, we tailor ADMM to our setting by introducing Bregman divergences to certain subproblems. Second, the optimization algorithm needs to solve an expensive equation that typically requires $O((m^2 + n^2) \times d^2)$ running time to invert two large matrices in each iteration. We provide a conjugate gradient (CG) based approach to obtain an *inexact* solution of this equation, using only $O(|\Omega| \times d)$ running time. As a result, our new method can significantly reduce the computation time (two orders of magnitude faster), as demonstrated in Appendix H.2. Notably, according to Theorem 2, we still guarantee the convergence using the inexact solutions during iterations.

Fully characterizing the statistical guarantee of the proposed class of penalty functions is challenging. Instead, we restrict to an important situation where the latent variables form a small number of subgroups. Specifically, we investigate a subgroup-based model, where two feature vectors in $\{\mathbf{x}_i^*\}$ or $\{\mathbf{y}_j^*\}$ are considered in the same group if they are identical. For a partially observed matrix corrupted with Gaussian noise, we prove that the complexity-regularized maximum likelihood estimator, as a special case of the framework (3), can achieve a lower error bound than the one for the trace-norm regularized matrix completion especially when the numbers of the subgroups for $\{\mathbf{x}_i^*\}$ and $\{\mathbf{y}_j^*\}$ are small. However, this estimator is computationally inefficient. To this end, we introduce a class of sparsity-promoting pairwise penalty functions (possibly with a finite support) to approximate the indicator function. Interestingly, not only can we identify the subgroups automatically but also we significantly reduce the recovery error, as verified in Section 5.3.

In addition, the theoretical analysis motivates us to adaptively construct the weights. As an application, our framework also applies to the datasets that do not provide side information since we heuristically pick adaptive weights based on the partially observed matrix. Our extensive experiments on both synthetic and real data demonstrate the superior performance of the proposed framework.

Notations: Let $\mathbf{A} = [A_{ij}] \in \mathbb{R}^{n \times m}$ be a $n \times m$ matrix and $\mathbf{x} = [x_1, \dots, x_n]^T \in \mathbb{R}^d$ be a d -dimensional vector. Denote by $|\mathcal{S}|$ the cardinality of a set \mathcal{S} . Recall the Frobenius norm $\|\mathbf{A}\|_F = (\sum_{ij} A_{ij}^2)^{\frac{1}{2}}$ and the infinity norm $\|\mathbf{A}\|_\infty = \max_{i,j} |A_{ij}|$. Define L_1 and L_2 norm as $\|\mathbf{x}\|_1 = \sum_{i=1}^d |x_i|$ and $\|\mathbf{x}\|_2 = (\sum_{i=1}^d x_i^2)^{\frac{1}{2}}$, respectively.

2 Optimization Framework

We develop a general optimization framework for (3) that allows a wide class of (non-)convex pairwise penalty functions $p(\mathbf{z}, \gamma)$, which are characterized by the following condition.

Condition 1. For any given vector $\mathbf{v} \in \mathbb{R}^d$, the penalty function $p(\mathbf{z}, \gamma)$ satisfies

1. $p(\mathbf{z}, \gamma) \geq 0$ for $\forall \mathbf{z} \in \mathbb{R}^d$,
2. there exists a constant $\varsigma_0 \geq 0$ independent of \mathbf{v} such that for $\forall \varsigma > \varsigma_0$, $f(\mathbf{z}) = \varsigma \|\mathbf{z} - \mathbf{v}\|_2^2 + p(\mathbf{z}, \gamma)$ is strongly convex with respect to $\mathbf{z} \in \mathbb{R}^d$.

This condition holds to a variety of (non-)convex pairwise penalty functions, including MCP (Zhang, 2010), M-type function and SCAD (Fan & Li, 2001). For example, Condition 1 holds for the MCP

$$p(\mathbf{z}, \gamma) = \gamma \|\mathbf{z}\|_2 - \frac{\|\mathbf{z}\|_2^2}{2t} \mathbf{1}(\|\mathbf{z}\|_2 \leq \gamma t) + \left(\frac{t\gamma^2}{2} - \gamma \|\mathbf{z}\|_2 \right) \mathbf{1}(\|\mathbf{z}\|_2 > \gamma t), \quad t > 0, \quad (4)$$

by setting $\varsigma_0 = 1/(2t)$, where $\mathbf{1}(\cdot)$ is the indicator function. Moreover, we introduce the following M-type function for our framework

$$p(\mathbf{z}, \gamma) = -\gamma (\|\mathbf{z}\|_2^2 - 2b\|\mathbf{z}\|_2) \mathbf{1}(\|\mathbf{z}\|_2 < 2b), \quad b > 0, \quad (5)$$

which satisfies Condition 1 by letting $\varsigma_0 = \gamma$. In addition, Condition 1 also holds for all convex functions, e.g., Lasso and the squared L_2 norm. Thus, our framework unifies the existing GRMF approaches.

3 Algorithm and Convergence

For the whole class of optimization problems introduced in Section 2, we develop an efficient and general algorithm, with a strong theoretical convergence guarantee. We begin with the following equivalent form of the main problem (3)

$$\begin{aligned} & \underset{\mathbf{X}, \mathbf{Y}}{\text{minimize}} \quad \frac{1}{2} \|\Psi_\Omega(\mathbf{M} - \mathbf{X}\mathbf{Y}^T)\|_F^2 + \frac{\alpha}{2} (\|\mathbf{X}\|_F^2 + \|\mathbf{Y}\|_F^2) \\ & \quad + \sum_{l \in \varepsilon_X} w_l p(\mathbf{p}_l, \gamma_X) + \sum_{l \in \varepsilon_Y} u_l p(\mathbf{q}_l, \gamma_Y) \\ & \text{subject to} \quad \mathbf{p}_l = \mathbf{x}_{l_1} - \mathbf{x}_{l_2}, \mathbf{q}_l = \mathbf{y}_{l_1} - \mathbf{y}_{l_2}, \end{aligned} \quad (6)$$

where the index set $\varepsilon_X = \{l = (l_1, l_2) : w_{l_1 l_2} > 0, l_1 < l_2\}$ and ε_Y is defined in a similar way for Y .

To express the constraints of (6) in a standard form, we introduce some notations. Let $l_x^i = (l_1^i, l_2^i) \in \varepsilon_X$ be an ordered sequence of index pairs such that $l_1^i \leq l_1^{i+1}$ and $l_1^i + l_2^i < l_1^{i+1} + l_2^{i+1}$ for any $1 \leq i \leq |\varepsilon_X| - 1$. Similarly, we can define $l_y^j \in \varepsilon_Y$. Moreover, define $\mathbf{P} \in \mathbb{R}^{d \times |\varepsilon_X|}$ with its i^{th} column vector being $\mathbf{P}_i = \mathbf{p}_{l_x^i}^T$ and $\mathbf{E}_x \in \mathbb{R}^{n \times |\varepsilon_X|}$ with its i^{th} column vector being $\mathbf{E}_x^i = \mathbf{e}_{l_1^i} - \mathbf{e}_{l_2^i}$, where the standard basis vector \mathbf{e}_k has a single non-zero value 1 at its k^{th} coordinate. Symmetrically, we can define matrices $\mathbf{Q} \in \mathbb{R}^{d \times |\varepsilon_Y|}$ and $\mathbf{E}_y \in \mathbb{R}^{m \times |\varepsilon_Y|}$. It can be verified that the standard form of the constraints of (6) is

$$\mathbf{P} - \mathbf{X}^T \mathbf{E}_x = \mathbf{0}, \quad \mathbf{Q} - \mathbf{Y}^T \mathbf{E}_y = \mathbf{0}. \quad (7)$$

Let $\mathcal{L}_\eta(\mathbf{P}, \mathbf{Q}, \mathbf{X}, \mathbf{Y}, \mathbf{\Lambda}, \mathbf{V})$ be the augmented Lagrangian function of the problem (6), which is given by

$$\begin{aligned} \mathcal{L}_\eta = & \frac{1}{2} \|\Psi_\Omega(\mathbf{M} - \mathbf{X}\mathbf{Y}^T)\|_F^2 + \frac{\alpha}{2} (\|\mathbf{X}\|_F^2 + \|\mathbf{Y}\|_F^2) + \text{tr}(\mathbf{\Lambda}^T (\mathbf{P} - \mathbf{X}^T \mathbf{E}_x)) + \text{tr}(\mathbf{V}^T (\mathbf{Q} - \mathbf{Y}^T \mathbf{E}_y)) \\ & + \frac{\eta}{2} (\|\mathbf{P} - \mathbf{X}^T \mathbf{E}_x\|_F^2 + \|\mathbf{Q} - \mathbf{Y}^T \mathbf{E}_y\|_F^2) + \sum_{i=1}^{|\varepsilon_X|} w_{l_x^i} p(\mathbf{P}_i, \gamma_X) + \sum_{j=1}^{|\varepsilon_Y|} u_{l_y^j} p(\mathbf{Q}_j, \gamma_Y), \end{aligned} \quad (8)$$

where the dual multiplier matrix $\mathbf{\Lambda} = [\mathbf{\Lambda}_1, \dots, \mathbf{\Lambda}_i, \dots, \mathbf{\Lambda}_{|\varepsilon_X|}]$ with $\mathbf{\Lambda}_i \in \mathbb{R}^d$ and $\mathbf{V} = [\mathbf{V}_1, \dots, \mathbf{V}_i, \dots, \mathbf{V}_{|\varepsilon_Y|}]$ with $\mathbf{V}_i \in \mathbb{R}^d$.

As commented in the introduction, the existing convergence results for the standard ADMM do not directly apply to our problem (6). Specifically, the row ranks of \mathbf{E}_x and \mathbf{E}_y in the constraints (7) are at most $n - 1$ and $m - 1$, respectively, contradicting the assumptions in Wang et al. (2015b) and (Hong et al., 2016) that require them to be both full row rank. The results in (Wang et al., 2015a) are not applicable either, because we also consider non-convex pairwise penalty functions. Next, we describe our 2-step algorithm based on a modified ADMM.

Step 1. Define an undirected graph $G_X = (V_X, E_X)$ with $V_X = \{1, 2, \dots, n\}$ and $E_X = \varepsilon_X$. We first use the standard depth-first-search algorithm to find cycles. Then, for each cycle of G_X , we randomly cut one edge l off by letting $w_l = 0$. As a result, the graph G_x becomes acyclic. Similar operations can be applied for $G_Y = (V_Y, E_Y)$. This step verifies Property 2 in Section 3.1, which guarantees the convergence of our algorithm.

Step 2. In each iteration k , we do the following updates:

$$\begin{aligned}
[1] \text{ Primal updates: } & \mathbf{P}^{k+1} = \arg \min_{\mathbf{P}} \mathcal{L}_\eta(\mathbf{P}, \mathbf{Q}^k, \mathbf{X}^k, \mathbf{Y}^k, \mathbf{\Lambda}^k, \mathbf{V}^k), \\
& \mathbf{Q}^{k+1} = \arg \min_{\mathbf{Q}} \mathcal{L}_\eta(\mathbf{P}^{k+1}, \mathbf{Q}, \mathbf{X}^k, \mathbf{Y}^k, \mathbf{\Lambda}^k, \mathbf{V}^k), \\
& \mathbf{X}^{k+1} = \arg \min_{\mathbf{X}} \left(\mathcal{L}_\eta(\mathbf{P}^{k+1}, \mathbf{Q}^{k+1}, \mathbf{X}, \mathbf{Y}^k, \mathbf{\Lambda}^k, \mathbf{V}^k) + \frac{1}{2} \|\mathbf{X} - \mathbf{X}^k\|_F^2 \right), \\
& \mathbf{Y}^{k+1} = \arg \min_{\mathbf{Y}} \left(\mathcal{L}_\eta(\mathbf{P}^{k+1}, \mathbf{Q}^{k+1}, \mathbf{X}^{k+1}, \mathbf{Y}, \mathbf{\Lambda}^k, \mathbf{V}^k) + \frac{1}{2} \|\mathbf{Y} - \mathbf{Y}^k\|_F^2 \right), \\
[2] \text{ Dual updates: } & \mathbf{\Lambda}^{k+1} = \mathbf{\Lambda}^k + \eta(\mathbf{P}^{k+1} - (\mathbf{X}^{k+1})^T \mathbf{E}_x), \\
& \mathbf{V}^{k+1} = \mathbf{V}^k + \eta(\mathbf{Q}^{k+1} - (\mathbf{Y}^{k+1})^T \mathbf{E}_y). \tag{9}
\end{aligned}$$

Remark on the modified ADMM: Compared to the standard ADMM, we introduce Bregman divergences to \mathbf{X}, \mathbf{Y} in (9). These additional terms guarantee sufficient descents of \mathcal{L}_η during the \mathbf{X}, \mathbf{Y} -subproblems in each iteration, as proven by Lemma 4 in Appendix C. Otherwise, the algorithm may diverge, as shown in Fig. 2¹. Compared to the Bregman ADMM (Wang & Banerjee, 2014), we do not apply Bregman divergences

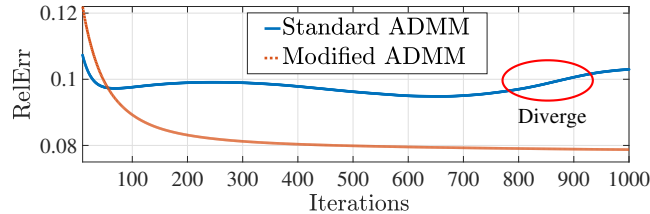


Figure 2: Illustration of the divergence by the standard ADMM applied to the optimization problem (6). We use MCP as the pairwise penalty function $p(\cdot, \gamma)$, and randomly pick 30% of the pixels of a 512×512 image *Lena* to generate the partially observed matrix $\Psi_\Omega(\mathbf{M})$. The relative error is defined by $\text{RelErr} = \|\widehat{\mathbf{M}} - \mathbf{M}\|_F / \|\mathbf{M}\|_F$, where $\widehat{\mathbf{M}}$ is the estimate.

to \mathbf{P} and \mathbf{Q} in order to save $O((|\varepsilon_X| + |\varepsilon_Y|) \times d)$ space for tracking \mathbf{P}^k and \mathbf{Q}^k .

Based on (9), updating \mathbf{P} in (8) is to solve the following proximal map for each of its column \mathbf{P}_i ,

$$\mathbf{P}_i^{k+1} = \arg \min_{\mathbf{P}_i} \left(\frac{1}{2} \|\mathbf{P}_i - \left((\mathbf{X}^k)^T \mathbf{E}_x^i - \eta^{-1} \mathbf{\Lambda}_i^k \right)\|_2^2 + \frac{w_{l_x}^i}{\eta} p(\mathbf{P}_i, \gamma_X) \right). \tag{10}$$

¹The image *Lena* was downloaded from http://www.utdallas.edu/~cxc123730/mh_bcs_spl.html

In practice, we choose $\eta > 2\zeta_0 w_{l_x^i}$, which, in conjunction with Condition 1, implies that the problem in (10) has a unique solution. Notably, this solution has simple and explicit analytical form for the pairwise penalty functions such as Lasso, SCAD, MCP and the M-type function.

Based on (9), updating \mathbf{X} is to minimize

$$F(\mathbf{X}) = \frac{1}{2} \sum_{(i,j) \in \Omega} (M_{ij} - \mathbf{x}_i(\mathbf{y}_j^k)^T)^2 + \frac{\eta}{2} \|\mathbf{P}^{k+1} - \mathbf{X}^T \mathbf{E}_x\|_F^2 \\ + \text{tr} \left((\mathbf{\Lambda}^k)^T \left(\mathbf{P}^{k+1} - \mathbf{X}^T \mathbf{E}_x \right) \right) + \frac{\alpha}{2} \|\mathbf{X}\|_F^2 + \frac{1}{2} \|\mathbf{X} - \mathbf{X}^k\|_F^2.$$

Proposition 1. *Minimizing $F(\mathbf{X})$ is equivalent to minimizing $f(\text{vec}(\mathbf{X}^T))$. The function $f(\mathbf{s})$, $\mathbf{s} \in \mathbb{R}^{nd}$ is defined by*

$$f(\mathbf{s}) = \frac{1}{2} \mathbf{s}^T (\mathbf{G}_y^k + (\eta \mathbf{E}_x \mathbf{E}_x^T + (\alpha + 1) \mathbf{I}_n) \otimes \mathbf{I}_d) \mathbf{s} - \mathbf{C} \mathbf{s}, \\ \mathbf{C} = \mathbf{b}_y^k + \text{vec}((\mathbf{X}^k)^T + \eta \mathbf{P}^{k+1} \mathbf{E}_x^T + \mathbf{\Lambda}^k \mathbf{E}_x^T)^T, \quad (11)$$

where $\mathbf{G}_y^k = \text{diag}(\mathbf{G}_1, \dots, \mathbf{G}_i, \dots, \mathbf{G}_n)$ is a block diagonal matrix with the i^{th} block $\mathbf{G}_i = \sum_{j \in \Omega_i} (\mathbf{y}_j^k)^T (\mathbf{y}_j^k) \in \mathbb{R}^{d \times d}$. The row vector $\mathbf{b}_y^k = [\mathbf{b}_1, \dots, \mathbf{b}_i, \dots, \mathbf{b}_n]$ satisfies $\mathbf{b}_i = \sum_{j \in \Omega_i} M_{ij} \mathbf{y}_j^k$, $\Omega_i = \{j : (i, j) \in \Omega\}$, with \mathbf{y}_j^k being the j^{th} row vector of the matrix \mathbf{Y}^k .

By Proposition 1, letting $\nabla_{\text{vec}(\mathbf{X}^T)} f(\text{vec}(\mathbf{X}^T)) = 0$ yields

$$(\mathbf{G}_y^k + (\eta \mathbf{E}_x \mathbf{E}_x^T + (\alpha + 1) \mathbf{I}_n) \otimes \mathbf{I}_d) \text{vec}(\mathbf{X}^T) = \mathbf{C}^T. \quad (12)$$

However, solving (12) requires inverting a $nd \times nd$ matrix, which is computationally demanding when dealing with large datasets. Motivated by (Rao et al., 2015), we use the standard CG to directly minimize $f(\text{vec}(\mathbf{X}^T))$.

The most expensive part in each iteration is the Hessian-vector multiplication $\nabla^2 f(\mathbf{s})\mathbf{s}$. Using the identity $(\mathbf{B}^T \otimes \mathbf{I}) \text{vec}(\mathbf{S}) = \text{vec}(\mathbf{S}\mathbf{B})$, we have

$$\nabla^2 f(\mathbf{s})\mathbf{s} = \mathbf{G}_y^k \mathbf{s} + \text{vec}(\eta \mathbf{S} \mathbf{E}_x \mathbf{E}_x^T + (\alpha + 1) \mathbf{S}), \quad (13)$$

where the matrix $\mathbf{S} = [\mathbf{s}_1, \dots, \mathbf{s}_n] \in \mathbb{R}^{d \times n}$ and $\mathbf{s} = \text{vec}(\mathbf{S})$. Since \mathbf{G}_y^k is a diagonal block matrix, computing $\mathbf{G}_y^k \mathbf{s}$ suffices to obtain $\mathbf{G}_i \mathbf{s}_i$, $1 \leq i \leq n$, which can be computed in $O(|\Omega_i|d)$ time by using $\mathbf{G}_i \mathbf{s}_i = \sum_{j \in \Omega_i} (\mathbf{y}_j^k \mathbf{s})(\mathbf{y}_j^k)^T$.

Thus, the time complexity for computing a single CG iteration is $O((|\Omega| + \text{nnz}(\mathbf{E}_x \mathbf{E}_x^T)) \times d)$, where $\text{nnz}(\cdot)$ is the number of non zeros. For our algorithm, we use a k_w -nearest neighbor method to select the weights w_{ij} , as introduced in section 4.3. Thus, using the structure of the matrix \mathbf{E}_x , we have an upper bound for $\text{nnz}(\mathbf{E}_x \mathbf{E}_x^T)$, as in the following proposition. Its proof is given in Appendix A.

Proposition 2. $\text{nnz}(\mathbf{E}_x \mathbf{E}_x^T) \leq n(k_w + 1)$.

In most real-world applications, k_w is small and satisfies $n(k_w + 1) < |\Omega|$. Thus, each CG iteration can be computed in $O(|\Omega| \times d)$ time. We stop CG if

$$\|\mathbf{A}_1 \text{vec}((\mathbf{X}^t)^T) - \mathbf{C}^T\|_2 \leq 10^3 \sqrt{dn} / (k + 1)^{0.6}, \quad (14) \\ \mathbf{A}_1 = \mathbf{G}_y^k + (\eta \mathbf{E}_x \mathbf{E}_x^T + (\alpha + 1) \mathbf{I}_n) \otimes \mathbf{I}_d,$$

Algorithm 1 Learning latent features with pairwise penalties in matrix completion by modified ADMM

```

1: Input:  $\Psi_\Omega(\mathbf{M}) \in \mathbb{R}^{n \times m}$ ,  $d \in \mathbb{N}^+$ ,  $\text{MaxIter} > 0$ ,  $\text{tol} > 0$ .
2: Initialize:  $\gamma_X, \gamma_Y, \alpha, \eta$ . Set  $\mathbf{X}, \mathbf{Y}, \mathbf{\Lambda}, \mathbf{V}$  as random matrices.
3: for  $k = 1$  to  $\text{MaxIter}$  do
4:   for  $i = 1$  to  $|\varepsilon_X|$  do
5:     Compute  $\mathbf{P}_i^{k+1}$  by solving the proximal map (10)
6:   end for
7:   for  $j = 1$  to  $|\varepsilon_Y|$  do
8:      $\mathbf{Q}_j^{k+1} = \arg \min_{\mathbf{Q}_j} \left( \frac{1}{2} \|\mathbf{Q}_j - ((\mathbf{Y}^k)^T \mathbf{E}_y^j - \frac{\mathbf{V}_j^k}{\eta})\|_2^2 + \frac{u_{ij}}{\eta} p(\mathbf{Q}_j, \gamma_Y) \right)$ 
9:   end for
10:  Update  $\mathbf{X}^{k+1}, \mathbf{Y}^{k+1}$  by minimizing (11) through CG
11:   $\mathbf{\Lambda}^{k+1} = \mathbf{\Lambda}^k + \eta (\mathbf{P}^{k+1} - (\mathbf{X}^{k+1})^T \mathbf{E}_x)$ 
12:   $\mathbf{V}^{k+1} = \mathbf{V}^k + \eta (\mathbf{Q}^{k+1} - (\mathbf{Y}^{k+1})^T \mathbf{E}_y)$ 
13:  if  $D_k < \text{tol}_1$  or  $|D_k - D_{k+1}| < \text{tol}_2$  then
14:    break and output  $\mathbf{X}^{k+1}$  and  $\mathbf{Y}^{k+1}$ 
15:  end if
16: end for
17: Output:  $\widehat{\mathbf{M}} = \mathbf{X}^{k+1} (\mathbf{Y}^{k+1})^T$ 

```

where \mathbf{X}^t is the output of the t^{th} CG iteration and the parameters on the right side are chosen to satisfy Theorem 2. Different from (Rao et al., 2015), we do not require CG to fully converge. Instead, we only need a very small number (≤ 5 in our implementation) of CG iterations to obtain an *inexact* solution $\widehat{\mathbf{X}}^{k+1}$ that satisfies (14), which still guarantees the convergence for our algorithm, as shown in Theorem 2. This step further speeds up our algorithm.

The main steps are provided in Algorithm 1, where $D_k = \|\widehat{\mathbf{X}}^k - \widehat{\mathbf{X}}^{k+1}\|_F / (2\sqrt{dn}) + \|\widehat{\mathbf{Y}}^k - \widehat{\mathbf{Y}}^{k+1}\|_F / (2\sqrt{dm})$ in the stop criterion. In the experiments, we choose $\text{tol}_1 = 10^{-1}$ and $\text{tol}_2 = 10^{-4}$.

Time complexity: The total time complexity for one iteration in Algorithm 1 is $O((|\Omega| + nnz(\mathbf{E}_x \mathbf{E}_x^T) + nnz(\mathbf{E}_y \mathbf{E}_y^T) + |\varepsilon_X| + |\varepsilon_Y|) \times d)$. Due to Step 1 and the weight selection, we usually have $|\varepsilon_X|d < |\Omega|$ and $|\varepsilon_Y|d < |\Omega|$. Thus, our algorithm is very efficient.

3.1 Convergence Guarantee

This section proves the convergence of our algorithm. Let $\mathbf{U}^k = (\mathbf{P}^k, \mathbf{Q}^k, \mathbf{X}^k, \mathbf{Y}^k, \mathbf{\Lambda}^k, \mathbf{V}^k)$ be the exact solutions of the subproblems in (9). We first prove the convergence of the sequence (\mathbf{U}^k) . Then, we extend this convergence result to Algorithm 1 that solves the equation (12) inexactly. We first provide two properties of our algorithm. Their proofs are presented in Appendix B.

Property 1 (Boundedness). *The sequence $(\mathbf{X}^k, \mathbf{Y}^k)$ generated by (9) is bounded. It means that there exist constants M_x, M_y such that $\|\mathbf{X}^k\|_F^2 \leq M_x, \|\mathbf{Y}^k\|_F^2 \leq M_y$.*

Property 2 (Full column rank). *After step 1 of the algorithm, the matrices \mathbf{E}_x and \mathbf{E}_y defined in (7) are both full column rank. Thus, there exist positive constants σ_x, σ_y such that $\mathbf{E}_x^T \mathbf{E}_x \succeq \sigma_x \mathbf{I}$ and $\mathbf{E}_y^T \mathbf{E}_y \succeq \sigma_y \mathbf{I}$.*

Using these two properties, we establish Lemma 2, 3 and 4 in Appendix C to upper bound the descent of \mathcal{L}_η during each subproblem. Based on these results, there exists a constant η_1 that is determined by $M_x, M_y, \sigma_x, \sigma_y$ such that

Theorem 1. *If $\eta > \eta_1$, then the sequence (\mathbf{U}^k) satisfies $\sum_{k=1}^{\infty} \|\mathbf{U}^{k+1} - \mathbf{U}^k\|_F^2 < \infty$ and converges to a*

stationary point of \mathcal{L}_η .

We refer to Appendix C for the proof. By Theorem 1, we extend the convergence result for inexact iterations. Let $\hat{\mathbf{U}}^k = (\mathbf{P}^k, \mathbf{Q}^k, \hat{\mathbf{X}}^k, \hat{\mathbf{Y}}^k, \mathbf{A}^k, \mathbf{V}^k)$ be the sequence generated by Algorithm 1. Define $\mathbf{t}_x^k = \mathbf{A}_1 \text{vec}((\hat{\mathbf{X}}^k)^T) - \mathbf{C}^T$ for $k \geq 1$, where matrices \mathbf{A}_1, \mathbf{C} are defined in (11). In a symmetric way, we can define \mathbf{t}_y^k . Following (He et al., 2015; Deng et al., 2017), we use the quantity $\|\hat{\mathbf{U}}^{k+1} - \hat{\mathbf{U}}^k\|_F^2$ as a measure of the convergence rate for the sequence $(\hat{\mathbf{U}}^k)$. Based on (14), we have $\sum_{k=1}^{\infty} \|\mathbf{t}_x^k\|_2^2 < \infty$ and $\sum_{k=1}^{\infty} \|\mathbf{t}_y^k\|_2^2 < \infty$. Then, we obtain

Theorem 2. *If $\eta > 2\eta_1$, then the sequence $(\hat{\mathbf{U}}^k)$ converges to a stationary point of \mathcal{L}_η . Furthermore, if the sequence $(\|\hat{\mathbf{U}}^{k+1} - \hat{\mathbf{U}}^k\|_F^2)$ is non-increasing, the convergence rate of Algorithm 1 is $o(1/k)$.*

The proof can be found in Appendix D. Different from the exact solution in Theorem 1, Theorem 2 only requires $\hat{\mathbf{X}}^k$ to satisfy $\sum_{k=1}^{\infty} \|\mathbf{t}_x^k\|_2^2 < \infty$. This extension allows more efficient methods to find inexact solutions of (12), e.g., the CG approach used in our algorithm. Interestingly, we observe that $\|\hat{\mathbf{U}}^{k+1} - \hat{\mathbf{U}}^k\|_F^2$ is non-increasing in most of our experiments. Thus, the $o(1/k)$ convergence rate is usually achievable in practice.

4 Statistical Properties

Fully characterizing the statistical guarantee of the proposed class of penalty functions in Section 2 is challenging. Instead, we restrict to an important subclass, which is used for the subgroup-based model. We can rigorously derive the estimation error bound for this class of penalty functions. More importantly, our theoretical analysis motivates two interesting directions for our framework, i.e., subgroup identification and adaptive weights. We first introduce the subgroup-based model in Section 4.1. Then, the estimation error is characterized in Section 4.2. This characterization directly motivates us to use adaptive weights in Section 4.3.

4.1 Subgroup-based Model

Assume that the ground truth $\mathbf{M}^* \in \mathbb{R}^{n \times m}$ can be factorized as $\mathbf{M}^* = \mathbf{X}^* \mathbf{Y}^{*T}$, where $\mathbf{X}^* \in \mathbb{R}^{n \times d}$, $\mathbf{Y}^* \in \mathbb{R}^{m \times d}$, and the observations $\Psi_\Omega(\mathbf{M}) = \Psi_\Omega(\mathbf{M}^* + \mathbf{N})$ are corrupted with the additive noise \mathbf{N} . The feature vectors $\{\mathbf{x}_i^*\}$ and $\{\mathbf{y}_j^*\}$ form some latent subgroups, where two features \mathbf{x}_i^* and \mathbf{x}_j^* (respectively \mathbf{y}_s^* and \mathbf{y}_t^*) are considered in the same subgroup if $\mathbf{x}_i^* = \mathbf{x}_j^*$ (respectively $\mathbf{y}_s^* = \mathbf{y}_t^*$). One key difference with the existing group based models, e.g., the group sparsity model (Kim et al., 2012), is that the subgroup structure in our model is not assumed to be known a priori. Studies (Jiacheng, 2017) have shown that the users with similar types in recommender systems often have the same feature, implying a natural subgroup structure. Nevertheless, our subgroup-based model is not restricted to these typical cases. For example, the number of subgroups can be even as large as the matrix dimension.

To facilitate the analysis, we introduce some useful notations. Let $\mathcal{G}(\mathbf{X}) = (\mathcal{G}_1^x, \dots, \mathcal{G}_{k_x}^x)$ and $\mathcal{G}(\mathbf{Y}) = (\mathcal{G}_1^y, \dots, \mathcal{G}_{k_y}^y)$ be two sets of mutually exclusive partitions of the indices $\{1, \dots, n\}$ and $\{1, \dots, m\}$, which satisfy $\mathbf{x}_i = \mathbf{x}_j$ for $\forall i, j \in \mathcal{G}_u^x, 1 \leq u \leq k_x$ and $\mathbf{y}_s = \mathbf{y}_t$ for $\forall s, t \in \mathcal{G}_v^y, 1 \leq v \leq k_y$. We use $|\mathcal{G}(\mathbf{X})| = k_x$ and $|\mathcal{G}(\mathbf{Y})| = k_y$ to denote the number of subgroups of $\{\mathbf{x}_i\}$ and $\{\mathbf{y}_j\}$, respectively.

4.2 Estimation Error Bound

This section derives the estimation error bound for the subgroup-based model. We first introduce the complexity-regularized maximum likelihood estimator, and show it is a special case of our framework. Then, we prove that this estimator achieves a lower bound compared to the standard trace-norm regularized matrix completion.

For an integer s with $s/(nm) \in (0, 1)$, assume that each index pair $(i, j) \in [n] \times [m]$ is included in the observed index set Ω independently with probability $s/(nm)$. The elements of the matrix $\Psi_\Omega(\mathbf{M})$ are independent conditional on the set Ω . The noise matrix \mathbf{N} contains i.i.d. random variables following a distribution $\mathcal{N}(0, \sigma^2)$. Assume $\|\mathbf{X}^*\|_\infty$, $\|\mathbf{Y}^*\|_\infty$ and $\|\mathbf{M}^*\|_\infty$ are bounded by C_x , C_y and C_m , respectively. First, we introduce the following complexity-regularized maximum likelihood estimator

$$\widehat{\mathbf{M}}(\Omega, \Phi_\Omega(\mathbf{M})) = \arg \min_{\mathbf{H} \in \mathcal{H}} \left\{ \|\Phi_\Omega(\mathbf{M} - \mathbf{H})\|_F^2 + \lambda(|\mathcal{G}(\mathbf{X})| + |\mathcal{G}(\mathbf{Y})|) \right\}, \quad (15)$$

where the finite set \mathcal{H} is given by

$$\mathcal{H} \triangleq \left\{ \mathbf{H} = \mathbf{X}\mathbf{Y}^T : \mathbf{X} \in \mathcal{X}, \mathbf{Y} \in \mathcal{Y}, \|\mathbf{H}\|_\infty \leq C_m \right\}. \quad (16)$$

The set \mathcal{X} in (16) is defined by

$$\mathcal{X} \triangleq \left\{ \mathbf{X} \in \mathbb{R}^{n \times d} : X_{ij} \in \left\{ -C_x + \frac{2C_x}{K}t, t = 0, 1, \dots, K-1 \right\} \right\} \quad (17)$$

with $K = 2^{\lceil \mu \log_2(n \vee m) \rceil}$, $(n \vee m) = \max(n, m)$, $\mu > 1$. In a symmetrical way, we can also define \mathcal{Y} .

Using the following proposition, we show that the estimator (15) is a special case of our framework (3).

Proposition 3. *Let K_i be the total number of the feature vectors \mathbf{x}_s that satisfy $\|\mathbf{x}_s - \mathbf{x}_i\|_2 < 2C_x/K$. We have, for $w_{ij} = 1/(K_i(n - K_i))$ and $\mathbf{X} \in \mathcal{X}$,*

$$|\mathcal{G}(\mathbf{X})| = \sum_{i,j} w_{ij} \Upsilon(\mathbf{x}_i - \mathbf{x}_j), \quad (18)$$

where the indicator function $\Upsilon(\mathbf{z}) = 0$ if $\|\mathbf{z}\|_2 < 2C_x/K$ and 1 otherwise. A symmetrical result holds for $|\mathcal{G}(\mathbf{Y})|$.

See Appendix E for the proof. Moreover, the constraints $\|\mathbf{X}\|_\infty \leq C_x$ and $\|\mathbf{Y}\|_\infty \leq C_y$ in (17) play a similar role as the regularizer $\alpha(\|\mathbf{X}\|_F^2 + \|\mathbf{Y}\|_F^2)/2$ in our framework. In the following theorem, we provide an error bound for the estimator (15).

Theorem 3. *If $\lambda \geq 8\mu d(\sigma^2 + 4C_m^2/3) \log(n \vee m)$, then the estimator (15) satisfies the error bound*

$$\begin{aligned} \frac{\mathbb{E} \left[\|\widehat{\mathbf{M}} - \mathbf{M}^*\|_F^2 \right]}{nm} &\leq \frac{C_1 \log s}{s} + \frac{dC_2}{(\mu \log(n \vee m))^2} + \left(\frac{6\lambda}{\log(n \vee m)} + \mu C_3 \right) \\ &\quad \left(\frac{(m+n+2)}{s} \log(n \vee m) + \frac{(|\mathcal{G}(\mathbf{X}^*)| + |\mathcal{G}(\mathbf{Y}^*)|)d}{s} \log(n \vee m) \right), \end{aligned} \quad (19)$$

where the expectation is with respect to the joint distribution of $(\Omega, \Phi_\Omega(\mathbf{M}))$ and C_1, C_2, C_3 are positive constants related to C_x, C_y and C_m .

The key step of the proof is the construction of the complexity penalty. See Appendix F for more details. We compare the error bound (19) with the one for the trace-norm regularized matrix completion obtained by (Koltchinskii et al., 2011), which assumes the observed entries are corrupted by additive noise. Casting Corollary 2 in (Koltchinskii et al., 2011) to our setting, we obtain an error bound

$$\frac{\|\widehat{\mathbf{M}} - \mathbf{M}^*\|_F^2}{nm} \leq c(\sigma^2 + t) \frac{(n+m)d}{s} \log(n \vee m) \quad (20)$$

with high probability, where c and t are two constants related to C_x , C_y and C_m . Note that our error bound

$$O\left(\left(|\mathcal{G}(\mathbf{X}^*)| + |\mathcal{G}(\mathbf{Y}^*)|\right)d + m + n\right) \log(n \vee m)/s$$

can be much lower than (20) provided that the total number of subgroups $|\mathcal{G}(\mathbf{X}^*)| + |\mathcal{G}(\mathbf{Y}^*)| \ll n + m$.

However, to directly optimize (15) with regularizer (18) is undesirable in practice since the indicator function complicates the optimization and the sets \mathcal{X}, \mathcal{Y} are discretized. Based on the analysis, we introduce the following heuristics:

- First, we undertake a slight relaxation of (15) by replacing \mathcal{X}, \mathcal{Y} with their convex hulls.
- Then, we use a class of sparsity-inducing penalty functions with finite support that can shrink some differences $\mathbf{x}_i - \mathbf{x}_j$ and $\mathbf{y}_s - \mathbf{y}_t$ to zeros, e.g., by MCP and SCAD, to approximate the indicator function. By checking whether a pair of feature vectors are equal or not, we can classify $\{\mathbf{x}_i\}$ and $\{\mathbf{y}_j\}$ into subgroups.
- Note that the formulation (18) encourages $\mathbf{x}_i \approx \mathbf{x}_j$ if $\mathbf{x}_i^* \approx \mathbf{x}_j^*$. Based on this observation, we introduce adaptive weights in Section 4.3.

Remarkably, not only can we identify the subgroups automatically but also we can significantly reduce the recovery error, as demonstrated in Section 5.3.

4.3 Adaptive Weights

Based on the discussion at the end of Section 4.2, we introduce the adaptive weights w_{ij} and u_{st} that are computed based on the partially observed matrix itself without any additional side information. The weights are chosen by

$$w_{ij} = \mathbf{I}_{ij}^{k_w} / d(\mathbf{x}_i^*, \mathbf{x}_j^*), \quad i \neq j \quad (21)$$

where the distance function $d(\mathbf{x}_i^*, \mathbf{x}_j^*)$ needs to be approximated and the indicator function $\mathbf{I}_{ij}^{k_w}$ is 1 if \mathbf{x}_j^* belongs to one of the k_w -nearest neighbors of \mathbf{x}_i^* and 0 otherwise. The selection (21) makes w_{ij} large during the computation if $\mathbf{x}_i^* \approx \mathbf{x}_j^*$, similar to the adaptive weight chosen in (Zou, 2006). It effectively pushes the optimization solver to return $\mathbf{x}_i \approx \mathbf{x}_j$. We also define u_{st} for \mathbf{y}_s and \mathbf{y}_t by replacing k_w and \mathbf{x} in (21) with k_v and \mathbf{y} , respectively. Thus, in the following we only explain w_{ij} . In practice, k_w and k_u are usually selected to be small, e.g., $k_w, k_u \leq 20$ in our experiments for collaborative filtering datasets. Below we provide two possible ways to estimate $d(\mathbf{x}_i^*, \mathbf{x}_j^*)$.

(I) For $\mathbf{M} = \mathbf{X}^* \mathbf{Y}^{*T} + \mathbf{N}$, assume that \mathbf{X}^* and \mathbf{Y}^* have full column rank d . Let σ_y be the smallest singular value of the matrix \mathbf{Y}^* . Define \mathbf{M}_i and \mathbf{N}_i as the i^{th} row vectors of \mathbf{M} and \mathbf{N} , respectively. Assume

that the noise is small such that $\|\mathbf{N}_i - \mathbf{N}_j\|_2 \ll \sigma_y$ for $1 \leq i < j \leq n$. Then, based on Remark 1 in (Li & Pong, 2015), we have $\sigma_y^2 \|\mathbf{x}_i^* - \mathbf{x}_j^*\|_2^2 \leq \|(\mathbf{x}_i^* - \mathbf{x}_j^*)(\mathbf{Y}^*)^T\|_2^2 = \|\mathbf{M}_i - \mathbf{M}_j - (\mathbf{N}_i - \mathbf{N}_j)\|_2^2 \leq 2\|\mathbf{M}_i - \mathbf{M}_j\|_2^2 + 2\|\mathbf{N}_i - \mathbf{N}_j\|_2^2$, which implies that if $\mathbf{M}_i \approx \mathbf{M}_j$, then \mathbf{x}_i^* is also very close to \mathbf{x}_j^* . Motivated by this simple observation, we define

$$d_1(\mathbf{x}_i^*, \mathbf{x}_j^*) = \left(\frac{\sum_{t \in \mathcal{S}_i \cap \mathcal{S}_j} (\mathbf{r}_i(t) - \mathbf{r}_j(t))^2}{|\mathcal{S}_i \cap \mathcal{S}_j|} \right)^{1/2} \quad (22)$$

where \mathbf{r}_i and \mathbf{r}_j are the i^{th} and j^{th} rows of the partially observed matrix $\Psi_\Omega(\mathbf{M})$ and the index set $\mathcal{S}_i = \{s \in \mathbb{N} : \mathbf{r}_i(s) \text{ is observed}\}$. Set $w_{ij} = 0$ if $\mathcal{S}_i \cap \mathcal{S}_j = \emptyset$.

(II) The second way is for the sparse collaborative filtering datasets. In this case, $d_1(\mathbf{x}_i^*, \mathbf{x}_j^*)$ is not a good choice since the number of observed common indices between the i^{th} and j^{th} rows (i.e., $|\mathcal{S}_i \cap \mathcal{S}_j|$) is too small to approximate the distance for many (i, j) . Thus, we define the distance in a two-step way. First, we define

$$d_2(\mathbf{x}_i^*, \mathbf{x}_j^*) = \left(\frac{\sum_{t \in \mathcal{S}_i \cup \mathcal{S}_j} (\bar{\mathbf{r}}_{i \rightarrow j}(t) - \bar{\mathbf{r}}_{j \rightarrow i}(t))^2}{|\mathcal{S}_i \cup \mathcal{S}_j|} \right)^{1/2} \quad (23)$$

where the vector $\bar{\mathbf{r}}_{i \rightarrow j}$ is defined by

$$\bar{\mathbf{r}}_{i \rightarrow j}(t) = \begin{cases} M_{t,i}, & t \in \mathcal{S}_i, \\ \sum_{r \in \mathcal{R}_t} M_{t,r} / |\mathcal{R}_t|, & t \in \mathcal{S}_j \setminus \mathcal{S}_i, \end{cases}$$

and \mathcal{R}_t is the set of indices of the observed entries for the t^{th} row of \mathbf{M} . Set $w_{ij} = 0$ if $\mathcal{S}_i \cup \mathcal{S}_j = \emptyset$. Using $d_2(\mathbf{x}_i^*, \mathbf{x}_j^*)$, we obtain a solution $\mathbf{X}^{(1)}$ and $\mathbf{Y}^{(1)}$ of the optimization problem (3) with weights computed by (21). Next, we use $\mathbf{X}^{(1)}$ and $\mathbf{Y}^{(1)}$ to compute the distance by $d(\mathbf{x}_i^*, \mathbf{x}_j^*) = \|\mathbf{x}_i^{(1)} - \mathbf{x}_j^{(1)}\|_2$.

5 Experiments

In this section, we first compare our algorithm to the classical MC (Candès & Recht, 2009) and two state-of-the-art GRMF algorithms, i.e., the graph regularized alternating Least Squares (GRALS) (Rao et al., 2015) and Separable Recurrent Multi-Graph CNN (sRMGCNN) (Monti et al., 2017) on different graphs. Then, we evaluate the effectiveness of the proposed adaptive weights. Finally, we use both synthetic and real datasets to verify our theoretical results in Section 4. We refer to our algorithm as LLMC. All experiments are performed using Matlab/Octave on a PC with macOS system, Intel 5 core 2.9 GHz CPU and 16G RAM. More empirical results can be found in Appendix H.

Real datasets: We conduct the experiments on two groups of collaborate filtering datasets: Jester² (Goldberg et al., 2001) and MovieLens³ (Harper & Konstan, 2016). Their statistics are presented in Appendix H.3. The jester datasets contain anonymous ratings of 100 jokes by users, where the ratings are real values ranging

²Jester datasets were downloaded from <http://goldberg.berkeley.edu/jester-data>

³MovieLens datasets were downloaded from <http://grouplens.org/datasets/movielens>

from -10.00 to 10.00. For MovieLen100k and MotiveLens1M datasets, the ratings of the movies have 5 scores (1-5).

Evaluation metric: For collaborate filtering datasets, we use the root mean square error (RMSE) to measure the prediction performance, given by $\text{RMSE} = \left(\sum_{i=1}^N (\hat{r}_i - r_i)^2 / N \right)^{1/2}$, where r_i is the observed rating in the test set, \hat{r}_i is the predicted rating and N is the total number of ratings in the test set.

Parameter selection: For our algorithm, we choose the regularization parameters γ_X and γ_Y from $2^{\{-2, \dots, 10\}}$, fix $\alpha = 1$ and set $\eta = 10^4$ to guarantee the convergence. In addition, we fix $d = 4$ for MovieLens datasets and $d = 100$ for Jester datasets. For MCP function (4), we select t from $\{0.5, 2, 20\}$, and for the M-type penalty function, we fix $b = 3$. We downloaded the code of **GRALS** from the author’s website⁴, and changed the number of iterations from 10 (default) to 100 to ensure the convergence.

5.1 Comparison to GRMF Algorithms

We test the performance of our proposed algorithm on real datasets. Following (Rao et al., 2015), we evaluate MovieLens100K using the five provided data splits. For MovieLens1M, we randomly split the observed ratings into a training set (90%) and a test set (10%). For jester datasets, we randomly choose 10% of the observed ratings as the training set and the remaining 90% as the test set. Table 1 summarizes the performance of different methods on the graphs that can cause the large penalty problem we discuss in the introduction. It shows that using MCP and M-type penalty, our method outperforms GRALS in all datasets. Table 2 shows that our method still makes improvement using the same graphs as in (Rao et al., 2015).

Table 1: RMSE on real datasets. We construct unweighted 100-nearest neighbor graphs for both users and movies using the distance metric (23)

Datasets	GRALS	LLFMC (MCP)	LLFMC (M-type)
Jester1	4.801	4.712	4.710
Jester2	4.880	4.831	4.838
Jester3	6.701	6.651	6.634
MovieLens100K	0.950	0.934	0.936
MovieLens1M	0.873	0.859	0.861

Table 2: RMSE on MovieLens100K. We use the same graphs as in (Rao et al., 2015) that were constructed by the side information.

Methods	MC	GRALS	sRMGCNN	LLFMC (M-type)	LLFMC (MCP)
RMSE	0.973	0.945	0.929	0.930	0.927

5.2 Performance of Adaptive Weights

Using the same setting as in Section 5.1, we test the performance of our proposed adaptive weights. We set $k_w = k_u = 10$ in our wights (21) for MovieLens datasets and set $k_w = 20, k_u = 2$ for Jester datasets. Based

⁴<http://nikrao.github.io/Code.html>

on the results in Table 1, Table 2 and Table 3, we make the following two observations. 1) Compared to the two kinds of weights used in Section 5.1 (including the weights constructed by the side information), the proposed adaptive weights significantly improve the performance of GRALS and our methods on all datasets. 2) Our method still outperforms the competitors in almost all experiments.

Table 3: RMSE on real datasets. For all datasets, we construct the graph based on our adaptive weights (21) using distance (23).

Datasets	GRALS	LLFMC (MCP)	LLFMC (M-type)
Jester1	4.713	4.651	4.672
Jester2	4.789	4.801	4.792
Jester3	6.461	6.551	6.461
MovieLens100K	0.919	0.909	0.914
MovieLens1M	0.851	0.847	0.850

5.3 Synthetic Data with Subgroups

To verify Theorem 3, we generate matrix $\mathbf{M}^* = \mathbf{X}^* \mathbf{Y}^{*T} \in \mathbb{R}^{n \times n}$, $\mathbf{X}^* \in \mathbb{R}^{n \times d}$, $\mathbf{Y}^* \in \mathbb{R}^{n \times d}$ in the following way. Let \mathbf{U}_1 be uniformly random in $[0, 1]^d$ and $\{\mathbf{U}_{i+1} - \mathbf{U}_i, 1 \leq i < k_x\}$ be i.i.d. and uniformly distributed on $[0, 10]^d$. Similarly we generate $\mathbf{V}_1, \dots, \mathbf{V}_{k_y}$. We evenly divide the feature vectors $\{\mathbf{x}_u^*\}$ into k_x subgroups and set the features in i^{th} subgroup to be \mathbf{U}_i . We divide $\{\mathbf{y}_v^*\}$ in a similar way. When $k_x = k_y = n$, there exist no subgroups. Multiplying by a constant, \mathbf{M}^* can satisfy $\|\mathbf{M}^*\|_F = 10^6$. The observed entries of $\Psi_\Omega(\mathbf{M})$ are sampled from $\mathbf{M} = \mathbf{M}^* + \mathbf{N}$ uniformly at random, with the noise \mathbf{N} containing i.i.d. elements following $\mathcal{N}(0, \sigma^2)$. Moreover, we use the first way (22) to compute the weights by setting $k_w = k_u = 0.15n$ and fix $d = 5$. Let $\widehat{\mathbf{M}}$ be the estimate of \mathbf{M}^* .

Relative error: We study three cases where the number of subgroups is small (20), medium (50) and large (200). Fig. 3 shows that our method significantly improves the recovery error, even though no real subgroups exist.

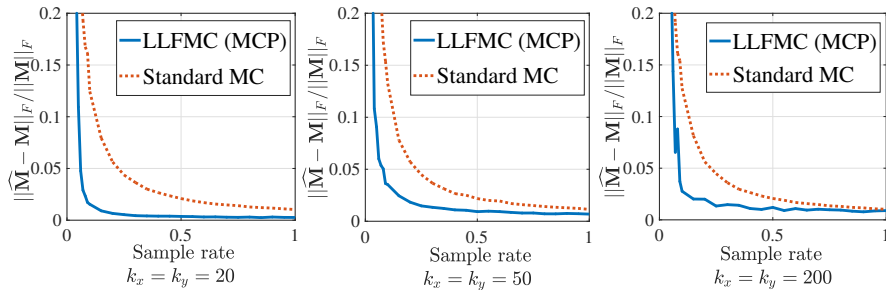


Figure 3: Relative error w.r.t. sample rate: $n = 200$, $\sigma = 10^2$.

Subgroup identification: Similar to (Han & Zhang, 2015), we provide the subgroups for the recovered features $\{\widehat{\mathbf{x}}_i\}$ and $\{\widehat{\mathbf{y}}_j\}$ by the matrices \mathbf{P} , \mathbf{Q} , where the features $\widehat{\mathbf{x}}_u$ and $\widehat{\mathbf{x}}_v$ (respectively $\widehat{\mathbf{y}}_s$ and $\widehat{\mathbf{y}}_t$) are in the same subgroup if and only if $P_{uv} = 1$ (respectively $Q_{st} = 1$). We choose $P_{uv} = 1$ if $\|\widehat{\mathbf{x}}_u - \widehat{\mathbf{x}}_v\|_2 < 0.01 \min\{\|\widehat{\mathbf{x}}_u\|_2, \|\widehat{\mathbf{x}}_v\|_2\}$ and 0 otherwise. Similarly, we can define the matrix \mathbf{Q} . Due to the limited space, we only virtualize the matrix \mathbf{P} in Fig. 4. The results clearly show that our method recovers the subgroup structure quite well. In contrast, the standard MC cannot identify this latent structure.

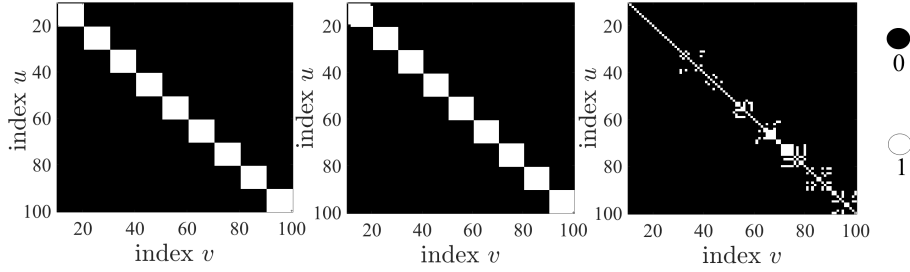


Figure 4: Illustration of matrix \mathbf{P} obtained by the ground truth (left), LFLMC (MCP) (middle) and the standard MC (right): $n = 100$, $\sigma = 100$, $k_x = k_y = 10$ and sample rate $\rho = 0.3$

5.4 Subgroup Identification for Real Dataset

We provide the subgroups of uses and movies from the MovieLens100K dataset computed by LFLMC (MCP). We use the adaptive weights (21) with the distance (23). Fig. 5 clearly shows that the users and movies exhibit subgroup structures; only 200 users and 200 movies are plotted for a better presentation. To get more useful information, we investigate the 2th largest user subgroup in Fig. 7 in detail. Interestingly, we find out that most users in this subgroup have ages between 25 and 35, consisting of mainly engineers and students.

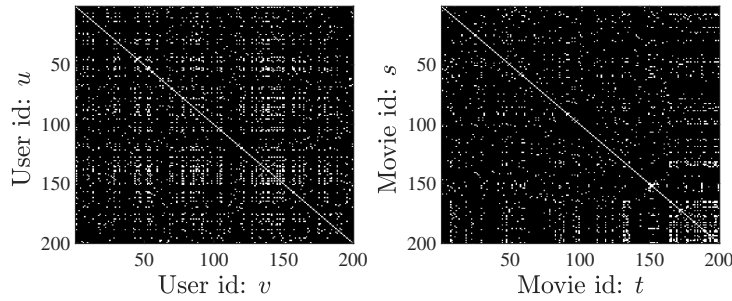


Figure 5: Illustration of \mathbf{P} (left) and \mathbf{Q} (right): $P_{uv} = 1$ (respectively $Q_{st} = 1$) (white spots) implies that user u and v (respectively movie s and t) are in the same subgroup.

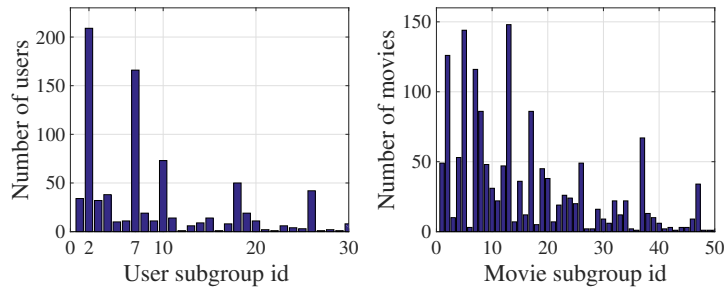


Figure 6: Subgroups (with more than one member): users and movies are divided into 62 and 87 subgroups, respectively.

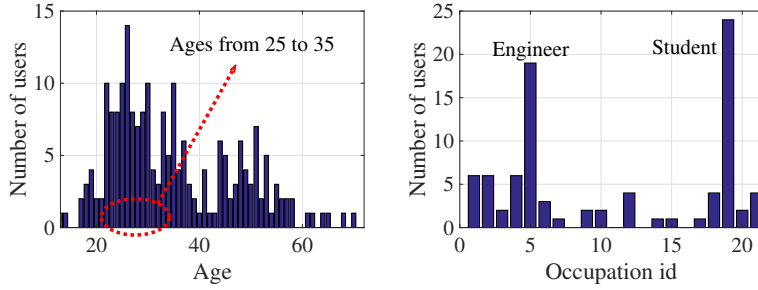


Figure 7: [Left] The age distribution in the 2^{th} largest user subgroup. [Right] The occupation distribution for the user ages between 25 and 35 in the 2^{th} largest user subgroup.

Table 4: Users in the 47^{th} user subgroup.

User id	Age	Occupation	Zip code
2	53	other	94043
29	41	programmer	94043
47	53	marketing	07102
53	26	programmer	55414
105	24	engineer	94043

Table 4 provides user information in a small subgroup with only 5 members. Interestingly, it shows that the majority live in the same area with related occupations.

6 Conclusion

We propose a new optimization framework to learn latent features in matrix completion by a wide class of (non-)convex pairwise penalty functions. To efficiently solve this class of optimization problems, we develop an efficient algorithm and prove its convergence guarantee. On the statistical guarantee, we characterize the complexity-regularized maximum likelihood estimator under the subgroup-based model. Extensive experiments on both synthetic and real data sets show the superior performance of our framework.

A Proof of Proposition 1 and 2

Proposition 1 can be directly obtained via some calculations based on the identities that $(\mathbf{B}^T \otimes \mathbf{A})\text{vec}(\mathbf{X}) = \text{vec}(\mathbf{A}\mathbf{X}\mathbf{B})$ and $\text{tr}(\mathbf{A}\mathbf{B}\mathbf{C}) = \text{vec}(\mathbf{A}^T)^T(\mathbf{I} \otimes \mathbf{B})\text{vec}(\mathbf{C})$. We now turn to prove Proposition 2. Recall the definition of the matrix \mathbf{E}_x given in Section 3 and let \mathbf{E}_i be the i^{th} row vector of the matrix \mathbf{E}_x . We then make the following three key observations for \mathbf{E}_x

1. Each \mathbf{E}_i has exactly k_w non zeros, $1 \leq i \leq n$.
2. For any two row vectors \mathbf{E}_i and \mathbf{E}_j , there exists at most one coordinate at which \mathbf{E}_i and \mathbf{E}_j are both non-zero.
3. Each column vector of the matrix \mathbf{E}_x has exactly two non zeros.

Based on these observations, we first claim that the row vector $\mathbf{E}_i \mathbf{E}_x^T = [\mathbf{E}_i \mathbf{E}_1^T, \mathbf{E}_i \mathbf{E}_2^T, \dots, \mathbf{E}_i \mathbf{E}_n^T]$ has at most $k_w + 1$ non zeros for $1 \leq i \leq n$. We then prove this result by contradiction. Without loss of generality, we consider the scenario where $i = 1$. Let $\{d_s, 1 \leq s \leq k_w\}$ be the coordinates at which \mathbf{E}_1 is non-zero. Suppose that the vector $\mathbf{E}_1 \mathbf{E}_x^T = [\mathbf{E}_1 \mathbf{E}_1^T, \dots, \mathbf{E}_1 \mathbf{E}_j^T, \dots, \mathbf{E}_1 \mathbf{E}_n^T]$ has $k_w + 2$ non zeros. Without loss of generality, we assume that $\mathbf{E}_1 \mathbf{E}_j^T \neq 0$ for $1 \leq j \leq k_w + 2$. Based on the observation 2 above, we have, for each $\mathbf{E}_j, 2 \leq j \leq k_w + 2$, there exists exactly one coordinate in $\{d_s, 1 \leq s \leq k_w\}$ at which \mathbf{E}_j is non-zero. Thus, there must exist one coordinate t in $\{d_s, 1 \leq s \leq k_w\}$ such that $\mathbf{E}_1(t) \neq 0, \mathbf{E}_u(t) \neq 0$ and $\mathbf{E}_v(t) \neq 0$, for certain $2 \leq u, v \leq k_w + 2$. However, this contradicts the observation 3. Thus, we conclude that the vector $\mathbf{E}_i \mathbf{E}_x^T$ has at most $k_w + 1$ non zeros. It means that $nnz(\mathbf{E}_i \mathbf{E}_x^T) \leq k_w + 1$ Then, using $\mathbf{E}_x \mathbf{E}_x^T = [(\mathbf{E}_1 \mathbf{E}_x^T)^T, (\mathbf{E}_2 \mathbf{E}_x^T)^T, \dots, (\mathbf{E}_n \mathbf{E}_x^T)^T]^T$ yields the proof.

B Proof of Properties

Property 1. Note that $\alpha(\|\mathbf{X}\|_F^2/2 + \|\mathbf{Y}\|_F^2)/2 \rightarrow \infty$ if $\|\mathbf{X}\|_F$ or $\|\mathbf{Y}\|_F \rightarrow \infty$. Then, using the coercivity of the objective function in (6), we have that, there exist $M_x, M_y \in \mathbb{R}^+$ such that $\|\mathbf{X}^k\|_F^2 \leq M_x, \|\mathbf{Y}^k\|_F^2 \leq M_y$ for $k \geq 1$. \square

Property 2. Recall that after step 1, the graph becomes acyclic. Note that \mathbf{E}_x is the incidence matrix associated to the graph $G_x = (V, E)$. Then, using Lemma 2.5 in (Bapat, 2010), we have that all columns $\mathbf{E}_x^1, \mathbf{E}_x^2, \dots, \mathbf{E}_x^{|\varepsilon_x|}$ of \mathbf{E}_x are linearly independent and hence \mathbf{E}_x is full column rank. Similar result holds for \mathbf{E}_y . Then, using Remark 1 in (Li & Pong, 2015), we finish the proof. \square

C Proof of Theorem 1

We first establish several lemmas, and then use these lemmas to prove Theorem 1.

Lemma 1. For any $\mathbf{A}_x \in \mathbb{R}^{d \times |\varepsilon_x|}$ and $\mathbf{A}_y \in \mathbb{R}^{d \times |\varepsilon_y|}$, we have $\|\mathbf{A}_x \mathbf{E}_x^T\|_F^2 \geq \sigma_x \|\mathbf{A}_x\|_F^2$ and $\|\mathbf{A}_y \mathbf{E}_y^T\|_F^2 \geq \sigma_y \|\mathbf{A}_y\|_F^2$.

Proof. Noting that $\mathbf{E}_x^T \mathbf{E}_x - \sigma_x \mathbf{I} \succeq 0$, we have $\|\mathbf{A} \mathbf{E}_x^T\|_F^2 - \sigma_x \|\mathbf{A}\|_F^2 = \text{tr}[\mathbf{A}(\mathbf{E}_x^T \mathbf{E}_x - \sigma_x \mathbf{I})\mathbf{A}^T] = \sum_{i=1}^d \mathbf{A}_x^i (\mathbf{E}_x^T \mathbf{E}_x - \sigma_x \mathbf{I}) (\mathbf{A}_x^i)^T \geq 0$, where \mathbf{A}_x^i is the i^{th} row vector of the matrix \mathbf{A}_x . Similarly, we can prove $\|\mathbf{A}_y \mathbf{E}_y^T\|_F^2 \geq \sigma_y \|\mathbf{A}_y\|_F^2$. \square

Lemma 2 (Upper bound the descents of multipliers). For each $k \in \mathbb{N}$, there exist a constant $L_y > 0$ such that

$$\begin{aligned} \|\Lambda^{k+1} - \Lambda^k\|_F^2 &\leq \frac{2}{\sigma_x} \|\mathbf{X}^k - \mathbf{X}^{k-1}\|_F^2 + \frac{2(M_x + 1)L_y}{\sigma_x} \|\mathbf{Y}^k - \mathbf{Y}^{k-1}\|_F^2 \\ &\quad + \frac{2L_y + 2(\alpha + 1)^2}{\sigma_x} \|\mathbf{X}^{k+1} - \mathbf{X}^k\|_F^2. \end{aligned} \quad (24)$$

Proof. Noting that $\text{vec}((\mathbf{X}^{k+1})^T)$ is the solution of the equation $\nabla_{\text{vec}(\mathbf{X}^T)} f(\text{vec}(\mathbf{X}^T)) = 0$ in (12), we obtain

$$(\mathbf{G}_y^k + (\eta \mathbf{E}_x \mathbf{E}_x^T + (\alpha + 1)) \otimes \mathbf{I}_d) \text{vec}((\mathbf{X}^{k+1})^T) = \mathbf{b}_y^k + \text{vec}((\mathbf{X}^k)^T) + \eta \mathbf{P}^{k+1} \mathbf{E}_x^T + \Lambda^k \mathbf{E}_x^T \quad (25)$$

which, together with $\mathbf{\Lambda}^{k+1} - \mathbf{\Lambda}^k = \eta(\mathbf{P}^{k+1} - (\mathbf{X}^{k+1})^T \mathbf{E}_x)$ and the identity $\text{vec}(\mathbf{AB}) = (\mathbf{B}^T \otimes \mathbf{I})\text{vec}(\mathbf{A})$, implies

$$\text{vec}(\mathbf{\Lambda}^{k+1} \mathbf{E}_x^T) = (\mathbf{G}_y^k + (\alpha + 1)\mathbf{I}_{nd})\text{vec}((\mathbf{X}^{k+1})^T) - (\mathbf{b}_y^k)^T - \text{vec}((\mathbf{X}^k)^T). \quad (26)$$

Using (26), we further obtain

$$\begin{aligned} \|(\mathbf{\Lambda}^{k+1} - \mathbf{\Lambda}^k) \mathbf{E}_x^T\|_F^2 &= \|\text{vec}((\mathbf{\Lambda}^{k+1} - \mathbf{\Lambda}^k) \mathbf{E}_x^T)\|_2^2 \\ &= \|(\mathbf{G}_y^k - \mathbf{G}_y^{k-1})\text{vec}((\mathbf{X}^{k+1})^T) + (\mathbf{b}_y^{k-1} - \mathbf{b}_y^k)^T + \mathbf{G}_y^{k-1}\text{vec}((\mathbf{X}^{k+1} - \mathbf{X}^k)^T) \\ &\quad + \text{vec}((\mathbf{X}^{k-1} - \mathbf{X}^k)^T) + (\alpha + 1)\text{vec}((\mathbf{X}^{k+1} - \mathbf{X}^k)^T)\|_2^2 \\ &\leq 2M_x \|\mathbf{G}_y^k - \mathbf{G}_y^{k-1}\|_F^2 + 2\|\mathbf{X}^{k-1} - \mathbf{X}^k\|_F^2 + 2(\alpha + 1)^2 \|\mathbf{X}^{k+1} - \mathbf{X}^k\|_F^2 \\ &\quad + 2\|\mathbf{b}_y^k - \mathbf{b}_y^{k-1}\|_2^2 + 2\|\mathbf{G}_y^{k-1}\|_F^2 \|\mathbf{X}^{k+1} - \mathbf{X}^k\|_F^2, \end{aligned} \quad (27)$$

where the inequality follows from the facts that $\|\mathbf{a} + \mathbf{b}\|_2^2 \leq (\|\mathbf{a}\|_2 + \|\mathbf{b}\|_2)^2 \leq 2(\|\mathbf{a}\|_2^2 + \|\mathbf{b}\|_2^2)$, $\|\mathbf{A}\mathbf{a}\|_2 \leq \|\mathbf{A}\|_F \|\mathbf{a}\|_2$ and $\|\mathbf{ab}\|_2 \leq \|\mathbf{a}\|_2 \|\mathbf{b}\|_2$. Recalling the definition of \mathbf{G}_y^k and \mathbf{b}_y^k in (11) and using Property 1, we have, there exists a sufficiently large constant L_y such that

$$\begin{aligned} \|\mathbf{G}_y^k\|_F^2 &\leq L_y, \|\mathbf{G}_y^k - \mathbf{G}_y^{k-1}\|_F^2 \leq L_y \|\mathbf{Y}^k - \mathbf{Y}^{k-1}\|_F^2 \\ \|\mathbf{b}_y^k\|_2^2 &\leq L_y, \|\mathbf{b}_y^k - \mathbf{b}_y^{k-1}\|_2^2 \leq L_y \|\mathbf{Y}^k - \mathbf{Y}^{k-1}\|_F^2, \end{aligned}$$

which, in conjunction with (27) and Lemma 1, completes the proof. \square

Using a similar approach as in Lemma 2, we have

$$\begin{aligned} \|\mathbf{V}^{k+1} - \mathbf{V}^k\|_F^2 &\leq \frac{2}{\sigma_y} \|\mathbf{Y}^k - \mathbf{Y}^{k-1}\|_F^2 + \frac{2(M_y + 1)L_x}{\sigma_y} \|\mathbf{X}^{k+1} - \mathbf{X}^k\|_F^2 \\ &\quad + \frac{2L_x + 2(\alpha + 1)^2}{\sigma_y} \|\mathbf{Y}^{k+1} - \mathbf{Y}^k\|_F^2. \end{aligned} \quad (28)$$

Define the constant $\eta_0 = 2\varsigma_0 \max(\widehat{w}, \widehat{u}) + 1$ with $\widehat{w} = \max_i \{w_{i_x}\}$ and $\widehat{u} = \max_j \{u_{i_j}\}$. Then we have

Lemma 3 (Upper bound the descents of \mathcal{L}_η during P, Q-subproblems). *Under Condition 1, we have, for any $\eta > \eta_0$ and each $k \in N$*

$$\mathcal{L}_\eta(\mathbf{P}^{k+1}, \mathbf{Q}^k, \mathbf{X}^k, \mathbf{Y}^k, \mathbf{\Lambda}^k, \mathbf{V}^k) - \mathcal{L}_\eta(\mathbf{P}^k, \mathbf{Q}^k, \mathbf{X}^k, \mathbf{Y}^k, \mathbf{\Lambda}^k, \mathbf{V}^k) \leq -\frac{\eta - \eta_0}{2} \|\mathbf{P}^{k+1} - \mathbf{P}^k\|_F^2.$$

Proof. Define the function $\tilde{p}(\mathbf{P}_i, \lambda_X) = w_{i_x} p(\mathbf{P}_i, \gamma_X) + \eta_0 \|\mathbf{P}_i - (\mathbf{X}^k)^T \mathbf{E}_x^i\|_2^2 / 2$. Recalling Condition 1 and noting $\eta_0 > 2\widehat{w}\varsigma_0$, we obtain $\tilde{p}(\mathbf{P}_i, \lambda_X)$ is strongly convex. Based on the optimality of \mathbf{P}_i^{k+1} for (10), we have

$$\mathbf{0} \in \partial_{\mathbf{P}_i} \tilde{p}(\mathbf{P}_i^{k+1}, \gamma_X) + \mathbf{\Lambda}_i^k + (\eta - \eta_0)(\mathbf{P}_i^{k+1} - (\mathbf{X}^k)^T \mathbf{E}_x^i).$$

Define $\mathbf{d}_k := -\mathbf{\Lambda}_i^k - (\eta - \eta_0)(\mathbf{P}_i^{k+1} - (\mathbf{X}^k)^T \mathbf{E}_x^i)$. Note that \mathbf{d}_k is a subgradient of the convex function $\tilde{p}(\mathbf{P}_i, \gamma_X)$ at $\mathbf{P}_i = \mathbf{P}_i^{k+1}$. Based on the definition of the subgradient of a convex function, we have

$$\tilde{p}(\mathbf{P}_i^k, \gamma_X) - \tilde{p}(\mathbf{P}_i^{k+1}, \gamma_X) \geq \langle \mathbf{d}_k, \mathbf{P}_i^k - \mathbf{P}_i^{k+1} \rangle. \quad (29)$$

Define a function $F_i(\mathbf{P}_i) = \tilde{p}(\mathbf{P}_i, \gamma_X) + (\boldsymbol{\Lambda}_i^k)^T (\mathbf{P}_i - (\mathbf{X}^k)^T \mathbf{E}_x^i) + (\eta - \eta_0) \|\mathbf{P}_i - (\mathbf{X}^k)^T \mathbf{E}_x^i\|_2^2 / 2$. Using (29), we have

$$\begin{aligned}
F_i(\mathbf{P}_i^{k+1}) - F_i(\mathbf{P}_i^k) &= \tilde{p}(\mathbf{P}_i^{k+1}, \gamma_X) - \tilde{p}(\mathbf{P}_i^k, \gamma_X) + \langle \boldsymbol{\Lambda}_i^k, \mathbf{P}_i^{k+1} - \mathbf{P}_i^k \rangle \\
&\quad - \frac{\eta - \eta_0}{2} \left(\|\mathbf{P}_i^k - (\mathbf{X}^k)^T \mathbf{E}_x^i\|_2^2 - \|\mathbf{P}_i^{k+1} - (\mathbf{X}^k)^T \mathbf{E}_x^i\|_2^2 \right) \\
&= \tilde{p}(\mathbf{P}_i^{k+1}, \gamma_X) - \tilde{p}(\mathbf{P}_i^k, \gamma_X) - \langle \mathbf{d}_k, \mathbf{P}_i^{k+1} - \mathbf{P}_i^k \rangle - \frac{\eta - \eta_0}{2} \|\mathbf{P}_i^{k+1} - \mathbf{P}_i^k\|_2^2, \\
&\leq -\frac{\eta - \eta_0}{2} \|\mathbf{P}_i^{k+1} - \mathbf{P}_i^k\|_2^2, \tag{30}
\end{aligned}$$

where the second equality follows from the cosine rule that $\|\mathbf{a} + \mathbf{c}\|_2^2 - \|\mathbf{b} + \mathbf{c}\|_2^2 = \|\mathbf{a} - \mathbf{b}\|_2^2 + 2\langle \mathbf{b} + \mathbf{c}, \mathbf{a} - \mathbf{b} \rangle$. Noting that $\sum_{i=1}^{|\varepsilon_X|} (\|\mathbf{P}_i^{k+1} - \mathbf{P}_i^k\|_2^2) = \|\mathbf{P}^{k+1} - \mathbf{P}^k\|_F^2$ and using (30), we have

$$\begin{aligned}
&\mathcal{L}_\eta(\mathbf{P}^{k+1}, \mathbf{Q}^k, \mathbf{X}^k, \mathbf{Y}^k, \boldsymbol{\Lambda}^k, \mathbf{V}^k) - \mathcal{L}_\eta(\mathbf{P}^k, \mathbf{Q}^k, \mathbf{X}^k, \mathbf{Y}^k, \boldsymbol{\Lambda}^k, \mathbf{V}^k) \\
&= \sum_{i=1}^{|\varepsilon_X|} \left(F_i(\mathbf{P}_i^{k+1}) - F_i(\mathbf{P}_i^k) \right) \leq -\frac{\eta - \eta_0}{2} \|\mathbf{P}^{k+1} - \mathbf{P}^k\|_F^2,
\end{aligned}$$

which finishes the proof. \square

By the symmetry of \mathbf{P} and \mathbf{Q} , we derive the similar results for \mathbf{Q} by replacing \mathbf{P} in Lemma 3 by \mathbf{Q} .

Lemma 4 (Upper bound the descents of \mathcal{L}_η of \mathbf{X} , \mathbf{Y} -subproblems). For $\forall k \in N$, we have

$$\begin{aligned}
&\mathcal{L}_\eta(\mathbf{P}^{k+1}, \mathbf{Q}^{k+1}, \mathbf{X}^{k+1}, \mathbf{Y}^{k+1}, \boldsymbol{\Lambda}^k, \mathbf{V}^k) - \mathcal{L}_\eta(\mathbf{P}^{k+1}, \mathbf{Q}^{k+1}, \mathbf{X}^k, \mathbf{Y}^k, \boldsymbol{\Lambda}^k, \mathbf{V}^k) \\
&\leq -\frac{1}{2} \left(\|\mathbf{X}^{k+1} - \mathbf{X}^k\|_F^2 + \|\mathbf{Y}^{k+1} - \mathbf{Y}^k\|_F^2 \right)
\end{aligned}$$

Proof. Since \mathbf{X}^{k+1} is the minimizer of the \mathbf{X} -subproblems in (9) respectively, we obtain

$$\begin{aligned}
&\mathcal{L}_\eta(\mathbf{P}^{k+1}, \mathbf{Q}^{k+1}, \mathbf{X}^{k+1}, \mathbf{Y}^k, \boldsymbol{\Lambda}^k, \mathbf{V}^k) + \frac{1}{2} \|\mathbf{X}^{k+1} - \mathbf{X}^k\|_F^2 \\
&\leq \mathcal{L}_\eta(\mathbf{P}^{k+1}, \mathbf{Q}^{k+1}, \mathbf{X}^k, \mathbf{Y}^k, \boldsymbol{\Lambda}^k, \mathbf{V}^k) + \frac{1}{2} \|\mathbf{X}^k - \mathbf{X}^k\|_F^2 = \mathcal{L}_\eta(\mathbf{P}^{k+1}, \mathbf{Q}^{k+1}, \mathbf{X}^k, \mathbf{Y}^k, \boldsymbol{\Lambda}^k, \mathbf{V}^k), \tag{31}
\end{aligned}$$

Similarly, we can obtain

$$\begin{aligned}
&\mathcal{L}_\eta(\mathbf{P}^{k+1}, \mathbf{Q}^{k+1}, \mathbf{X}^{k+1}, \mathbf{Y}^{k+1}, \boldsymbol{\Lambda}^k, \mathbf{V}^k) + \frac{1}{2} \|\mathbf{Y}^{k+1} - \mathbf{Y}^k\|_F^2 \\
&\leq \mathcal{L}_\eta(\mathbf{P}^{k+1}, \mathbf{Q}^{k+1}, \mathbf{X}^{k+1}, \mathbf{Y}^k, \boldsymbol{\Lambda}^k, \mathbf{V}^k) + \frac{1}{2} \|\mathbf{Y}^k - \mathbf{Y}^k\|_F^2 = \mathcal{L}_\eta(\mathbf{P}^{k+1}, \mathbf{Q}^{k+1}, \mathbf{X}^{k+1}, \mathbf{Y}^k, \boldsymbol{\Lambda}^k, \mathbf{V}^k), \tag{32}
\end{aligned}$$

Combing (31) and (32) yields the proof. \square

To prove the main theorem, we introduce some notations.

$$\begin{aligned}
\sigma_0 &= \frac{2}{\eta\sigma_x}, \sigma_1 = \frac{2(M_x + 1)L_y}{\eta\sigma_x} + \frac{2}{\eta\sigma_y}, \sigma_2 = \frac{1}{2} - \frac{2L_y + 2(\alpha + 1)^2}{\eta\sigma_x} - \frac{2(M_y + 1)L_x}{\eta\sigma_y}, \\
\sigma_3 &= \frac{1}{2} - \frac{2L_x + 2(\alpha + 1)^2}{\eta\sigma_y}, \sigma_* = \min \left\{ \frac{\eta - \eta_0}{2}, \sigma_2 - \sigma_0, \sigma_3 - \sigma_1 \right\}. \tag{33}
\end{aligned}$$

proof of Theorem 1. Based on 8, we have

$$\begin{aligned}
& \mathcal{L}_\eta(\mathbf{P}^{k+1}, \mathbf{Q}^{k+1}, \mathbf{X}^{k+1}, \mathbf{Y}^{k+1}, \mathbf{\Lambda}^{k+1}, \mathbf{V}^{k+1}) - \mathcal{L}_\eta(\mathbf{P}^{k+1}, \mathbf{Q}^{k+1}, \mathbf{X}^{k+1}, \mathbf{Y}^{k+1}, \mathbf{\Lambda}^k, \mathbf{V}^k) \\
&= \text{tr} \left((\mathbf{\Lambda}^{k+1} - \mathbf{\Lambda}^k)^T (\mathbf{P}^{k+1} - (\mathbf{X}^{k+1})^T \mathbf{E}_x) \right) + \text{tr} \left((\mathbf{V}^{k+1} - \mathbf{V}^k)^T (\mathbf{Q}^{k+1} - (\mathbf{Y}^{k+1})^T \mathbf{E}_y) \right) \\
&= \frac{1}{\eta} \|\mathbf{\Lambda}^{k+1} - \mathbf{\Lambda}^k\|_F^2 + \frac{1}{\eta} \|\mathbf{V}^{k+1} - \mathbf{V}^k\|_F^2.
\end{aligned} \tag{34}$$

where the last equality follows from the dual updates that

$$\mathbf{\Lambda}^{k+1} - \mathbf{\Lambda}^k = \eta (\mathbf{P}^{k+1} - (\mathbf{X}^{k+1})^T \mathbf{E}_x) \text{ and } \mathbf{V}^{k+1} - \mathbf{V}^k = \eta (\mathbf{Q}^{k+1} - (\mathbf{Y}^{k+1})^T \mathbf{E}_y). \tag{35}$$

Combining (24), (28), (34), Lemma 3 and Lemma 4, we have

$$\begin{aligned}
\mathcal{L}_\eta(\mathbf{U}^{k+1}) - \mathcal{L}_\eta(\mathbf{U}^k) &\leq -\frac{\eta - \eta_0}{2} \left(\|\mathbf{P}^{k+1} - \mathbf{P}^k\|_F^2 + \|\mathbf{Q}^{k+1} - \mathbf{Q}^k\|_F^2 \right) \\
&\quad + \sigma_0 \|\mathbf{X}^k - \mathbf{X}^{k-1}\|_F^2 + \sigma_1 \|\mathbf{Y}^k - \mathbf{Y}^{k-1}\|_F^2 \\
&\quad - \sigma_2 \|\mathbf{X}^{k+1} - \mathbf{X}^k\|_F^2 - \sigma_3 \|\mathbf{Y}^{k+1} - \mathbf{Y}^k\|_F^2.
\end{aligned} \tag{36}$$

Let $\tilde{\mathbf{U}}^k = (\mathbf{P}^k, \mathbf{Q}^k, \mathbf{X}^k, \mathbf{Y}^k, \mathbf{\Lambda}^k, \mathbf{V}^k, \mathbf{X}^{k-1}, \mathbf{Y}^{k-1})$ and define $\hat{\mathcal{L}}_\eta$ as

$$\hat{\mathcal{L}}_\eta(\tilde{\mathbf{U}}^k) = \mathcal{L}_\eta(\mathbf{U}^k) + \sigma_0 \|\mathbf{X}^k - \mathbf{X}^{k-1}\|_F^2 + \sigma_1 \|\mathbf{Y}^k - \mathbf{Y}^{k-1}\|_F^2, \tag{37}$$

which, in conjunction with (36), indicates that

$$\begin{aligned}
\hat{\mathcal{L}}_\eta(\tilde{\mathbf{U}}^{k+1}) - \hat{\mathcal{L}}_\eta(\tilde{\mathbf{U}}^k) &\leq -\frac{\eta - \eta_0}{2} \left(\|\mathbf{P}^{k+1} - \mathbf{P}^k\|_F^2 + \|\mathbf{Q}^{k+1} - \mathbf{Q}^k\|_F^2 \right) \\
&\quad - (\sigma_2 - \sigma_0) \|\mathbf{X}^{k+1} - \mathbf{X}^k\|_F^2 - (\sigma_3 - \sigma_1) \|\mathbf{Y}^{k+1} - \mathbf{Y}^k\|_F^2 \\
&\leq -\sigma_* \left(\|\mathbf{P}^{k+1} - \mathbf{P}^k\|_F^2 - \|\mathbf{Q}^{k+1} - \mathbf{Q}^k\|_F^2 + \|\mathbf{X}^{k+1} - \mathbf{X}^k\|_F^2 \right. \\
&\quad \left. + \|\mathbf{Y}^{k+1} - \mathbf{Y}^k\|_F^2 \right).
\end{aligned} \tag{38}$$

Consider a constant

$$\eta_1 = \max \left\{ \frac{4 + 4L_y + 4(\alpha + 1)^2}{\sigma_x} + \frac{4(M_y + 1)L_x}{\sigma_y}, \frac{4L_x + 4(\alpha + 1)^2}{\sigma_y} + \frac{4(M_x + 1)L_y}{\sigma_x}, \eta_0 + \frac{1}{4} \right\}. \tag{39}$$

Combining (33) and (39), we have $\sigma_* > 0$ for any $\eta > \eta_1$, which implies that $\hat{\mathcal{L}}_\eta(\tilde{\mathbf{U}}^k)$ is non-increasing.

Next, we show that the sequences (\mathbf{U}^k) and $(\tilde{\mathbf{U}}^k)$ are bounded. The boundedness of the sequence $(\mathbf{X}^k, \mathbf{Y}^k)$ follows from Property 1. Recalling (26) and using Property 1, we obtain

$$\|\mathbf{\Lambda}^k\|_F^2 \leq \frac{2(M_x + 1)L_y + 2M_x + 2(\alpha + 1)^2 M_x}{\sigma_x} \tag{40}$$

A symmetric result holds for $\|\mathbf{V}^k\|_F^2$. Thus, the sequence $(\mathbf{\Lambda}^k, \mathbf{V}^k)$ is bounded. Based on the definition of $\widehat{\mathcal{L}}_\eta(\widetilde{\mathbf{U}}^k)$ in (37) and the non-negativity of $p(\cdot, \gamma)$, we have

$$\begin{aligned}
\widehat{\mathcal{L}}_\eta(\widetilde{\mathbf{U}}^k) &\geq \frac{1}{2} \|\Psi_\Omega(\mathbf{X}^k(\mathbf{Y}^k)^T - \mathbf{M})\|_F^2 - \frac{1}{2\eta} \left(\|\mathbf{\Lambda}^k\|_F^2 + \|\mathbf{V}^k\|_F^2 \right) \\
&\quad + \frac{\eta}{2} \|\mathbf{P}^k - (\mathbf{X}^k)^T \mathbf{E}_x + \frac{1}{\eta} \mathbf{\Lambda}^k\|_F^2 + \frac{\alpha}{2} \left(\|\mathbf{X}^k\|_F^2 + \|\mathbf{Y}^k\|_F^2 \right) \\
&\quad + \frac{\eta}{2} \|\mathbf{Q}^k - (\mathbf{Y}^k)^T \mathbf{E}_y + \frac{1}{\eta} \mathbf{V}^k\|_F^2 + \sigma_0 \|\mathbf{X}^k - \mathbf{X}^{k-1}\|_F^2 + \sigma_1 \|\mathbf{Y}^k - \mathbf{Y}^{k-1}\|_F^2 \\
&\geq \frac{\eta}{2} \|\mathbf{P}^k - (\mathbf{X}^k)^T \mathbf{E}_x + \frac{1}{\eta} \mathbf{\Lambda}^k\|_F^2 - \frac{1}{2\eta} \left(\|\mathbf{\Lambda}^k\|_F^2 + \|\mathbf{V}^k\|_F^2 \right) \\
&\quad + \frac{\eta}{2} \|\mathbf{Q}^k - (\mathbf{Y}^k)^T \mathbf{E}_y + \frac{1}{\eta} \mathbf{V}^k\|_F^2. \tag{41}
\end{aligned}$$

Since $\widehat{\mathcal{L}}_\eta(\widetilde{\mathbf{U}}^k)$ is non-increasing, we have $\widehat{\mathcal{L}}_\eta(\widetilde{\mathbf{U}}^1) \geq \widehat{\mathcal{L}}_\eta(\widetilde{\mathbf{U}}^k)$ for $\forall k \in \mathbb{N}$, which, in conjunction with (41), shows that

$$\begin{aligned}
&\frac{\eta}{2} \|\mathbf{P}^k - (\mathbf{X}^k)^T \mathbf{E}_x + \frac{1}{\eta} \mathbf{\Lambda}^k\|_F^2 + \frac{\eta}{2} \|\mathbf{Q}^k - (\mathbf{Y}^k)^T \mathbf{E}_y + \frac{1}{\eta} \mathbf{V}^k\|_F^2 \\
&\leq \widehat{\mathcal{L}}_\eta(\widetilde{\mathbf{U}}^1) + \frac{1}{2\eta} \|\mathbf{\Lambda}^k\|_F^2 + \frac{1}{2\eta} \|\mathbf{V}^k\|_F^2 < \infty.
\end{aligned}$$

Then, based on the boundedness of $(\mathbf{X}^k, \mathbf{Y}^k, \mathbf{\Lambda}^k, \mathbf{V}^k)$ and the properties of Frobenius norm that $\|\mathbf{A} - \mathbf{B}\|_F \geq \|\mathbf{A}\|_F - \|\mathbf{B}\|_F$ and $\|\mathbf{AB}\|_F \leq \|\mathbf{A}\|_F \|\mathbf{B}\|_F$, we further obtain

$$\|\mathbf{P}^k\|_F \leq \|\mathbf{X}^k\|_F \|\mathbf{E}_x\|_F + \frac{1}{\eta} \|\mathbf{\Lambda}^k\|_F < \infty, \quad \|\mathbf{Q}^k\|_F \leq \|\mathbf{Y}^k\|_F \|\mathbf{E}_y\|_F + \frac{1}{\eta} \|\mathbf{V}^k\|_F < \infty,$$

which implies that the sequence $(\mathbf{P}^k, \mathbf{Q}^k)$ is bounded. Combining the results above yields the boundedness of the sequences (\mathbf{U}^k) and $(\widetilde{\mathbf{U}}^k)$.

Since $(\widetilde{\mathbf{U}}^k)$ is bounded, there exists a subsequence $(\widetilde{\mathbf{U}}^{k_i}, i \geq 1)$ that converges to $\widetilde{\mathbf{U}}^*$. By the continuity of the function $\widehat{\mathcal{L}}_\eta$, we obtain $\liminf_{i \rightarrow \infty} \widehat{\mathcal{L}}_\eta(\widetilde{\mathbf{U}}^{k_i}) \geq \widehat{\mathcal{L}}_\eta(\widetilde{\mathbf{U}}^*)$, which, together with that $\widehat{\mathcal{L}}_\eta(\widetilde{\mathbf{U}}^k)$ is non-increasing, implies that the sequences $(\widehat{\mathcal{L}}_\eta(\widetilde{\mathbf{U}}^{k_i}))$ and $(\widehat{\mathcal{L}}_\eta(\widetilde{\mathbf{U}}^k))$ are bounded below by $\widehat{\mathcal{L}}_\eta(\widetilde{\mathbf{U}}^*)$.

Using the inequality (38), we have, for a fixed $n \in \mathbb{N}$,

$$\begin{aligned}
&\sigma_* \sum_{k=1}^n \left(\|\mathbf{P}^{k+1} - \mathbf{P}^k\|_F^2 + \|\mathbf{Q}^{k+1} - \mathbf{Q}^k\|_F^2 + \|\mathbf{X}^{k+1} - \mathbf{X}^k\|_F^2 + \|\mathbf{Y}^{k+1} - \mathbf{Y}^k\|_F^2 \right) \\
&\leq \sum_{k=1}^n \left(\widehat{\mathcal{L}}_\eta(\widetilde{\mathbf{U}}^k) - \widehat{\mathcal{L}}_\eta(\widetilde{\mathbf{U}}^{k+1}) \right) \leq \widehat{\mathcal{L}}_\eta(\widetilde{\mathbf{U}}^1) - \widehat{\mathcal{L}}_\eta(\widetilde{\mathbf{U}}^*) < \infty, \tag{42}
\end{aligned}$$

which, in conjunction with (24) and (28), indicates that $\sum_{k=1}^\infty \|\mathbf{U}^{k+1} - \mathbf{U}^k\|_F^2 < \infty$ and $\lim_{k \rightarrow \infty} \|\mathbf{U}^{k+1} - \mathbf{U}^k\|_F^2 \rightarrow 0$. Let $\mathbf{U}^* = (\mathbf{P}^*, \mathbf{Q}^*, \mathbf{X}^*, \mathbf{Y}^*, \mathbf{\Lambda}^*, \mathbf{V}^*)$ denote the limit point of the sequence (\mathbf{U}^k) . Applying

Fermat's rule to (9) yields

$$\begin{aligned}
\mathbf{0} &= \nabla_{\mathbf{X}} \left(\frac{1}{2} \|\Psi_{\Omega}(\mathbf{X}^{k+1}(\mathbf{Y}^k)^T - \mathbf{M})\|_F^2 + \frac{\alpha}{2} \|\mathbf{X}^{k+1}\|_F^2 \right) + \mathbf{E}_x(\boldsymbol{\Lambda}^k)^T \\
&\quad + \left(\mathbf{X}^{k+1} - \mathbf{X}^k \right) - \eta \mathbf{E}_x \left((\mathbf{P}^{k+1})^T - \mathbf{E}_x^T \mathbf{X}^{k+1} \right), \\
\mathbf{0} &= \nabla_{\mathbf{Y}} \left(\frac{1}{2} \|\Psi_{\Omega}(\mathbf{X}^{k+1}(\mathbf{Y}^{k+1})^T - \mathbf{M})\|_F^2 + \frac{\alpha}{2} \|\mathbf{Y}^{k+1}\|_F^2 \right) + \mathbf{E}_y(\mathbf{V}^k)^T \\
&\quad + \left(\mathbf{Y}^{k+1} - \mathbf{Y}^k \right) - \eta \mathbf{E}_y \left((\mathbf{Q}^{k+1})^T - \mathbf{E}_y^T \mathbf{Y}^{k+1} \right), \\
\mathbf{0} &\in \partial_{\mathbf{P}} \sum_{i=1}^{|\varepsilon_X|} w_{l_i} p(\mathbf{P}_i^{k+1}, \gamma_X) + \boldsymbol{\Lambda}^k + \eta \left(\mathbf{P}^{k+1} - (\mathbf{X}^k)^T \mathbf{E}_x \right), \\
\mathbf{0} &\in \partial_{\mathbf{Q}} \sum_{j=1}^{|\varepsilon_Y|} u_{l_j} p(\mathbf{Q}_j^{k+1}, \gamma_Y) + \mathbf{V}^k + \eta \left(\mathbf{Q}^{k+1} - (\mathbf{Y}^k)^T \mathbf{E}_y \right). \tag{43}
\end{aligned}$$

Recalling the dual updates that

$$\boldsymbol{\Lambda}^{k+1} - \boldsymbol{\Lambda}^k = \eta \left(\mathbf{P}^{k+1} - (\mathbf{X}^{k+1})^T \mathbf{E}_x \right) \text{ and } \mathbf{V}^{k+1} - \mathbf{V}^k = \eta \left(\mathbf{Q}^{k+1} - (\mathbf{Y}^{k+1})^T \mathbf{E}_y \right)$$

and using (43) and $\lim_{k \rightarrow \infty} \|\mathbf{U}^{k+1} - \mathbf{U}^k\|_F^2 \rightarrow 0$, we obtain $\mathbf{P}^* - (\mathbf{X}^*)^T \mathbf{E}_x = \mathbf{0}$, $\mathbf{Q}^* - (\mathbf{Y}^*)^T \mathbf{E}_y = \mathbf{0}$ and

$$\begin{aligned}
\mathbf{0} &\in \partial_{\mathbf{P}} \sum_{i=1}^{|\varepsilon_X|} w_{l_i} p(\mathbf{P}_i^*, \gamma_X) + \boldsymbol{\Lambda}^*, \quad \mathbf{0} \in \partial_{\mathbf{Q}} \sum_{j=1}^{|\varepsilon_Y|} u_{l_j} p(\mathbf{Q}_j^*, \gamma_Y) + \mathbf{V}^*, \\
\mathbf{0} &= \nabla_{\mathbf{X}} \left(\frac{1}{2} \|\Psi_{\Omega}(\mathbf{X}^*(\mathbf{Y}^*)^T - \mathbf{M})\|_F^2 + \frac{\alpha}{2} \|\mathbf{X}^*\|_F^2 \right) + \mathbf{E}_x(\boldsymbol{\Lambda}^*)^T, \\
\mathbf{0} &= \nabla_{\mathbf{Y}} \left(\Psi_{\Omega} \left(\frac{1}{2} \|\mathbf{X}^*(\mathbf{Y}^*)^T - \mathbf{M}\|_F^2 + \frac{\alpha}{2} \|\mathbf{Y}^*\|_F^2 \right) \right) + \mathbf{E}_y(\mathbf{V}^*)^T,
\end{aligned}$$

which implies that $\mathbf{0} \in \partial \mathcal{L}_{\eta}(\mathbf{U}^*)$ and thus \mathbf{U}^* is a stationary point of \mathcal{L}_{η} . \square

D Proof of Theorem 2

Proof. Note that $\widehat{\mathbf{X}}^{k+1}$ can be regarded as the minimizer of the following subproblem

$$\widehat{\mathbf{X}}^{k+1} = \arg \min_{\mathbf{X}} \left(f(\text{vec}(\mathbf{X}^T)) - (\mathbf{t}_x^{k+1})^T \text{vec}(\mathbf{X}^T) \right), \tag{44}$$

where the function $f(\cdot)$ is given by (11). Then, using a similar approach to (26), we can obtain

$$\text{vec}(\boldsymbol{\Lambda}^{k+1} \mathbf{E}_x^T) = (\mathbf{G}_y^k + (\alpha + 1) \mathbf{I}_{nd}) \text{vec}((\widehat{\mathbf{X}}^{k+1})^T) - (\mathbf{b}_y^k)^T - \mathbf{t}_x^{k+1} - \text{vec}((\widehat{\mathbf{X}}^k)^T). \tag{45}$$

Similar to (24) and based on (45), we have

$$\begin{aligned}
\|\boldsymbol{\Lambda}^{k+1} - \boldsymbol{\Lambda}^k\|_F^2 &\leq \frac{2}{\sigma_x} \|\widehat{\mathbf{X}}^k - \widehat{\mathbf{X}}^{k-1}\|_F^2 + \frac{2(M_x + 1)L_y}{\sigma_x} \|\mathbf{Y}^k - \mathbf{Y}^{k-1}\|_F^2 \\
&\quad + \frac{2L_y + 2(\alpha + 1)^2}{\sigma_x} \|\widehat{\mathbf{X}}^{k+1} - \widehat{\mathbf{X}}^k\|_F^2 \\
&\quad + \frac{2}{\sigma_x} \left(\|\mathbf{t}_x^k\|_2^2 + \|\mathbf{t}_x^{k+1}\|_2^2 \right) \tag{46}
\end{aligned}$$

A symmetrical result holds for $\|\mathbf{V}^{k+1} - \mathbf{V}^k\|_F^2$. Using a similar approach to (31) and recalling (44), we have

$$\begin{aligned}
& \mathcal{L}_\eta(\mathbf{P}^{k+1}, \mathbf{Q}^{k+1}, \widehat{\mathbf{X}}^{k+1}, \widehat{\mathbf{Y}}^k, \boldsymbol{\Lambda}^k, \mathbf{V}^k) - \mathcal{L}_\eta(\mathbf{P}^{k+1}, \mathbf{Q}^{k+1}, \mathbf{X}^k, \mathbf{Y}^k, \boldsymbol{\Lambda}^k, \mathbf{V}^k) \\
& \leq -\frac{1}{2} \|\widehat{\mathbf{X}}^{k+1} - \widehat{\mathbf{X}}^k\|_F^2 + \mathbf{t}_x^{k+1} (\text{vec}(\widehat{\mathbf{X}}^{k+1}) - \text{vec}(\widehat{\mathbf{X}}^k)) \\
& \leq -\frac{1}{4} \|\widehat{\mathbf{X}}^{k+1} - \widehat{\mathbf{X}}^k\|_F^2 + \frac{1}{2} \|\mathbf{t}_x^{k+1}\|_2^2.
\end{aligned} \tag{47}$$

where the last inequality follows from the fact that $\|\mathbf{A} + \mathbf{B}\|_F^2 \leq 2(\|\mathbf{A}\|_F^2 + \|\mathbf{B}\|_F^2)$. A symmetrical result holds for $\widehat{\mathbf{Y}}^{k+1}$. Next, we show that the sequence $(\widehat{\mathbf{U}}^k)$ is bounded. The boundedness of $(\widehat{\mathbf{X}}^k, \widehat{\mathbf{Y}}^k)$ follows from Property 1. Similar to (40), using (45) and Property 1 yields the boundedness of $(\boldsymbol{\Lambda}^k, \mathbf{V}^k)$, which, in conjunction with the last two equalities in (9), yields the boundedness of $(\mathbf{P}^k, \mathbf{Q}^k)$. These facts imply the boundedness of the sequence of $(\widehat{\mathbf{U}}^k)$.

Since the function $\widehat{\mathcal{L}}_\eta$ is continuous and coercive, by the boundedness of $(\widehat{\mathbf{U}}^k)$, we have, there exists $M_l > 0$ such that $|\widehat{\mathcal{L}}_\eta(\widehat{\mathbf{U}}^k)| < M_l$ for $\forall k$. Combining (47), Lemma 3 and Lemma 4, we have

$$\begin{aligned}
& \left(\sigma_* - \frac{1}{4}\right) \sum_{k=1}^n \left(\|\mathbf{P}^{k+1} - \mathbf{P}^k\|_F^2 + \|\mathbf{Q}^{k+1} - \mathbf{Q}^k\|_F^2 + \|\widehat{\mathbf{X}}^{k+1} - \widehat{\mathbf{X}}^k\|_F^2 + \|\widehat{\mathbf{Y}}^{k+1} - \widehat{\mathbf{Y}}^k\|_F^2 \right) \\
& \leq \widehat{\mathcal{L}}_\eta(\widehat{\mathbf{U}}^1) - \widehat{\mathcal{L}}_\eta(\widehat{\mathbf{U}}^{n+1}) + \frac{1}{2} \sum_{k=1}^{n+1} \left(\|\mathbf{t}_x^k\|_2^2 + \|\mathbf{t}_y^k\|_2^2 \right) \\
& \leq 2M_l + \frac{1}{2} \sum_{k=1}^{\infty} \|\mathbf{t}_x^k\|_2^2 + \frac{1}{2} \sum_{k=1}^{\infty} \|\mathbf{t}_y^k\|_2^2 < \infty.
\end{aligned} \tag{48}$$

Combining (39), (33) and $\eta > 2\eta_1$, we have $\sigma_* > 1/4$. Then, letting $n \rightarrow \infty$ in (48) implies

$$\sum_{k=1}^{\infty} \left(\|\mathbf{P}^{k+1} - \mathbf{P}^k\|_F^2 + \|\mathbf{Q}^{k+1} - \mathbf{Q}^k\|_F^2 + \|\widehat{\mathbf{X}}^{k+1} - \widehat{\mathbf{X}}^k\|_F^2 + \|\widehat{\mathbf{Y}}^{k+1} - \widehat{\mathbf{Y}}^k\|_F^2 \right) < \infty, \tag{49}$$

which, in conjunction with that $\sum_{k=1}^{\infty} \|\mathbf{t}_x^k\|_2^2 < \infty$ and (46), implies that $\sum_{k=1}^{\infty} \|\boldsymbol{\Lambda}^{k+1} - \boldsymbol{\Lambda}^k\|_F^2 < \infty$. Similarly, we can obtain $\sum_{k=1}^{\infty} \|\mathbf{V}^{k+1} - \mathbf{V}^k\|_F^2 < \infty$. Thus, we have $\lim_{k \rightarrow \infty} \|\widehat{\mathbf{U}}^{k+1} - \widehat{\mathbf{U}}^k\|_F^2 = 0$.

Let $\widehat{\mathbf{U}}^* = (\mathbf{P}^*, \mathbf{Q}^*, \widehat{\mathbf{X}}^*, \widehat{\mathbf{Y}}^*, \boldsymbol{\Lambda}^*, \mathbf{V}^*)$ be a cluster point of $\{\widehat{\mathbf{U}}^k\}$. Applying Fermat's rule to (44), we obtain

$$\begin{aligned}
\mathbf{0} = & \nabla_{\widehat{\mathbf{X}}} \left(\frac{1}{2} \|\Psi_\Omega(\widehat{\mathbf{X}}^{k+1}(\widehat{\mathbf{Y}}^k)^T - \mathbf{M})\|_F^2 + \frac{\alpha}{2} \|\widehat{\mathbf{X}}^{k+1}\|_F^2 \right) \\
& + \mathbf{E}_x(\boldsymbol{\Lambda}^k)^T - \eta \mathbf{E}_x \left((\mathbf{P}^{k+1})^T - (\mathbf{E}_x)^T \widehat{\mathbf{X}}^{k+1} \right) \\
& + \left(\widehat{\mathbf{X}}^{k+1} - \widehat{\mathbf{X}}^k - \mathbf{T}_x^{k+1} \right),
\end{aligned} \tag{50}$$

and have two identities

$$\mathbf{P}^* - (\widehat{\mathbf{X}}^*)^T \mathbf{E}_x = \mathbf{0} \quad \text{and} \quad \mathbf{Q}^* - (\widehat{\mathbf{Y}}^*)^T \mathbf{E}_y = \mathbf{0}, \tag{51}$$

where $\text{vec}((\mathbf{T}_x^{k+1})^T) = \mathbf{t}_x^{k+1}$. Combining (50), (51), $\lim_{k \rightarrow \infty} \|\widehat{\mathbf{U}}^{k+1} - \widehat{\mathbf{U}}^k\|_F \rightarrow 0$ and $\lim_{k \rightarrow \infty} \|\mathbf{t}_x^{k+1}\|_2 = 0$, we can obtain

$$\begin{aligned} \mathbf{0} &= \nabla_{\widehat{\mathbf{X}}} \left(\frac{1}{2} \|\Psi_{\Omega}(\widehat{\mathbf{X}}^* (\widehat{\mathbf{Y}}^*)^T - \mathbf{M})\|_F^2 + \frac{\alpha}{2} \|\widehat{\mathbf{X}}^*\|_F^2 \right) + \mathbf{E}_x(\mathbf{\Lambda}^*)^T, \\ \mathbf{0} &= \nabla_{\widehat{\mathbf{Y}}} \left(\frac{1}{2} \|\Psi_{\Omega}(\widehat{\mathbf{X}}^* (\widehat{\mathbf{Y}}^*)^T - \mathbf{M})\|_F^2 + \frac{\alpha}{2} \|\widehat{\mathbf{Y}}^*\|_F^2 \right) + \mathbf{E}_y(\mathbf{V}^*)^T, \\ \mathbf{0} &\in \partial_{\mathbf{P}} \sum_{i=1}^{|\varepsilon_X|} w_{l_i} p(\mathbf{P}_i^*, \gamma_X) + \mathbf{\Lambda}^*, \\ \mathbf{0} &\in \partial_{\mathbf{Q}} \sum_{j=1}^{|\varepsilon_Y|} u_{l_j} p(\mathbf{Q}_j^*, \gamma_Y) + \mathbf{V}^*. \end{aligned}$$

Thus, we have $\mathbf{0} \in \partial \mathcal{L}_{\eta}(\widehat{\mathbf{U}}^*)$ and $\widehat{\mathbf{U}}^*$ is a stationary point of \mathcal{L}_{η} .

According to (49), we have $\sum_{k=1}^{\infty} \|\widehat{\mathbf{U}}^{k+1} - \widehat{\mathbf{U}}^k\|_F^2 < \infty$. Thus, if the sequence $(\|\widehat{\mathbf{U}}^{k+1} - \widehat{\mathbf{U}}^k\|_F^2)$ is non-increasing, we have

$$2k \|\widehat{\mathbf{U}}^{2k+1} - \widehat{\mathbf{U}}^{2k}\|_F^2 \leq 2 \sum_{i=k+1}^{2k} \|\widehat{\mathbf{U}}^{i+1} - \widehat{\mathbf{U}}^i\|_F^2 \rightarrow 0$$

as $k \rightarrow \infty$. Thus, we have $\|\widehat{\mathbf{U}}^{k+1} - \widehat{\mathbf{U}}^k\|_F^2 = o(1/k)$. \square

E Proof of Proposition 3

Suppose $i \in \mathcal{G}_{s_i}^x$ for certain $1 \leq s_i \leq k_x$. Based on the definition (17), we have $\|\mathbf{x}_j - \mathbf{x}_i\|_2 < 2C_x/K$ for any $j \in \mathcal{G}_{s_i}^x$ and $\|\mathbf{x}_j - \mathbf{x}_i\|_2 \geq 2C_x/K$ for any $j \in (\mathcal{G}_{s_i}^x)^c = \bigcup_{1 \leq t \leq k_x, t \neq s_i} \mathcal{G}_t^x$. According to the definition of K_i , we have $|(\mathcal{G}_{s_i}^x)^c| = n - K_i$. Using these facts, we have

$$\sum_{j=1}^n \frac{\Upsilon(\mathbf{x}_i - \mathbf{x}_j)}{K_i(n - K_i)} = \left(\sum_{j \in \mathcal{G}_{s_i}^x} + \sum_{j \in (\mathcal{G}_{s_i}^x)^c} \right) \frac{\Upsilon(\mathbf{x}_i - \mathbf{x}_j)}{K_i(n - K_i)} = 0 + \sum_{j \in (\mathcal{G}_{s_i}^x)^c} \frac{1}{K_i(n - K_i)} = \frac{1}{K_i},$$

which implies

$$\sum_{i,j} w_{ij} \Upsilon(\mathbf{x}_i - \mathbf{x}_j) = \sum_{i=1}^n \sum_{j=1}^n \frac{1}{K_i(n - K_i)} \Upsilon(\mathbf{x}_i - \mathbf{x}_j) = \sum_{i=1}^n \frac{1}{K_i} = k_x = |\mathcal{G}(\mathbf{X})| \quad (52)$$

where the third equality in (52) follows from the fact that $K_i = K_j$ for any $i, j \in \mathcal{G}_s^x, 1 \leq s \leq k_x$.

F Proof of Theorem 3

Let $p(x)$ and $q(x)$ denote the pdf of a real-valued random variable x . Recall the Kullback-Leibler divergence $D(p||q) \triangleq \mathbb{E}_p[\log(p(x)/q(x))]$ and the Hellinger affinity $A(p, q) \triangleq \mathbb{E}_p[\sqrt{q(x)/p(x)}]$. We first quote the following lemma.

Lemma 5 (Lemma A.1 in [Soni et al. \(2014\)](#)). Let \mathbf{M}^* be a $n \times m$ target matrix we aim to reconstruct and let \mathcal{H} be a finite collection of candidate estimates \mathbf{H} of \mathbf{M}^* , each with a penalty $\text{pen}(\mathbf{H}) \geq 1$ such that $\sum_{\mathbf{H} \in \mathcal{H}} 2^{-\text{pen}(\mathbf{H})} \leq 1$. Fix an integer s with $1 \leq s \leq nm$, let $\gamma = s/(nm)$. Each $(i, j) \in [n] \times [m]$ is included in the observed index set Ω with probability γ . Assume that the joint pdf of the observations $\Phi_\Omega(\mathbf{M})$ follows $p_{\mathbf{M}^*}(\Phi_\Omega(\mathbf{M})) = \prod_{(i,j) \in \Omega} p_{M_{ij}^*}(M_{ij})$, which are assumed to be independent conditional on Ω .

Given a constant C_D satisfying

$$C_D \geq \max_{\mathbf{H} \in \mathcal{H}} \max_{(i,j) \in [n] \times [m]} \mathbf{D}(p_{M_{ij}^*}(M_{ij}) || p_{H_{ij}}(M_{ij})), \quad (53)$$

we have that for any $\xi \geq (1 + 2C_D/3) 2 \log 2$, the complexity regularized maximum likelihood estimator

$$\widehat{\mathbf{M}} = \widehat{\mathbf{M}}(\Omega, \Phi_\Omega(\mathbf{M})) = \arg \min_{\mathbf{H} \in \mathcal{H}} \{-\log p_{\mathbf{H}}(\Phi_\Omega(\mathbf{M})) + \xi \text{pen}(\mathbf{H})\} \quad (54)$$

satisfies the estimation error bound

$$\begin{aligned} \frac{\mathbb{E}[-2 \log A(p_{\widehat{\mathbf{M}}}(\mathbf{M}), p_{\mathbf{M}^*}(\mathbf{M}))]}{nm} &\leq \frac{8C_D \log s}{s} + 3 \min_{\mathbf{H} \in \mathcal{H}} \left\{ \frac{\mathbf{D}(p_{\mathbf{M}^*}(\mathbf{M}) || p_{\mathbf{H}}(\mathbf{M}))}{nm} \right. \\ &\quad \left. + \left(\xi + \frac{4C_D \log 2}{3} \right) \frac{\text{pen}(\mathbf{H})}{s} \right\}, \end{aligned} \quad (55)$$

where the expectation is with respect to the joint distribution of $(\Omega, \Phi_\Omega(\mathbf{M}))$ and the shorthands

$$\begin{aligned} A(p_{\widehat{\mathbf{M}}}(\mathbf{M}), p_{\mathbf{M}^*}(\mathbf{M})) &= \prod_{i,j \in [n] \times [m]} A(p_{\widehat{M}_{ij}}(M_{ij}), p_{M_{ij}^*}(M_{ij})), \\ \mathbf{D}(p_{\mathbf{M}^*}(\mathbf{M}) || p_{\mathbf{H}}(\mathbf{M})) &= \sum_{i,j \in [n] \times [m]} \mathbf{D}(p_{M_{ij}^*}(M_{ij}) || p_{H_{ij}}(M_{ij})). \end{aligned} \quad (56)$$

Main step. To use this lemma, we need to construct penalties $\text{pen}(\mathbf{H})$ for each $\mathbf{H} \in \mathcal{H}$ defined in (16) such that the Kraft's inequality $\sum_{\mathbf{H} \in \mathcal{H}} 2^{-\text{pen}(\mathbf{H})} \leq 1$ holds. Let $\mathcal{H}_1 \triangleq \{\mathbf{H} = \mathbf{X}\mathbf{Y}^T : \mathbf{X} \in \mathcal{X}, \mathbf{Y} \in \mathcal{Y}\}$, where \mathcal{X} and \mathcal{Y} are defined in (17). Based on ([Cover & Thomas, 2012](#)), the inequality $\sum_{\mathbf{H} \in \mathcal{H}_1} 2^{-\text{pen}(\mathbf{H})} \leq 1$ can be satisfied by choosing $\text{pen}(\mathbf{H})$ to be the code length of some uniquely decodable binary code for each $\mathbf{H} \in \mathcal{H}_1$. Thus, we use the following three steps to design $\text{pen}(\mathbf{H})$. Recall $K = 2^{\lceil \mu \log_2(\max\{n,m\}) \rceil}$, $\mu > 1$. For simple notations, we let $n_0 = \max\{n, m\}$.

1. We first encode the number of subgroups of $\{\mathbf{x}_i, 1 \leq i \leq n\}$, i.e., $|\mathcal{G}(\mathbf{X})|$, with $\lceil \log_2(n) \rceil$ bits. Similarly, encode $|\mathcal{G}(\mathbf{Y})|$ with $\lceil \log_2(m) \rceil$ bits.
2. For each $\mathbf{x}_i, 1 \leq i \leq n$, we encode the index of the subgroup \mathbf{x}_i belongs to with $\lceil \log_2(n) \rceil$ bits. Similarly, for each $\mathbf{y}_j, 1 \leq j \leq m$, we encode the index of the subgroup \mathbf{y}_j belongs to with $\lceil \log_2(m) \rceil$ bits. Thus, the total number of bits used in this step is $n \lceil \log_2(n) \rceil + m \lceil \log_2(m) \rceil$.
3. Finally, based on (17), we encode each value X_{ij} with $\log_2(K)$ bits. Similarly, we encode Y_{ij} with $\log_2(K)$ bits. Since all row vectors in a subgroup are identical, the total number of bits used in this step is $d \log_2(K) (|\mathcal{G}(\mathbf{X})| + |\mathcal{G}(\mathbf{Y})|)$.

4. We assign each $\mathbf{H} \in \mathcal{H}_1$ with a code that is concatenation of the code for \mathbf{X} followed by the code for \mathbf{Y} . Then, note that

$$\text{pen}(\mathbf{H}) = (n+1)\lceil \log_2(n) \rceil + (m+1)\lceil \log_2(m) \rceil + d \log_2(K)(|\mathcal{G}(\mathbf{X})| + |\mathcal{G}(\mathbf{Y})|) \quad (57)$$

is the code length of the unique code assigned to $\mathbf{H} \in \mathcal{H}_1$. Since such codes are uniquely decodable, we have $\sum_{\mathbf{H} \in \mathcal{H}_1} 2^{-\text{pen}(\mathbf{H})} \leq 1$.

Noting that $\mathcal{H} \subseteq \mathcal{H}_1$, we have $\sum_{\mathbf{H} \in \mathcal{H}} 2^{-\text{pen}(\mathbf{H})} \leq \sum_{\mathbf{H} \in \mathcal{H}_1} 2^{-\text{pen}(\mathbf{H})} \leq 1$. Then, by replacing $\text{pen}(\mathbf{H})$ in Lemma 5 by (57), our estimate is given by

$$\widehat{\mathbf{M}} = \arg \min_{\mathbf{H} \in \mathcal{H}} \left\{ -\log p_{\mathbf{H}}(\Phi_{\Omega}(\mathbf{M})) + \xi d \log_2(K)(|\mathcal{G}(\mathbf{X})| + |\mathcal{G}(\mathbf{Y})|) \right\}, \quad (58)$$

which, based on the fact that $\max\{\lceil \log_2(n) \rceil, \lceil \log_2(m) \rceil\} \leq \log_2(K) = \lceil \mu \log_2(n_0) \rceil$, satisfies

$$\begin{aligned} \frac{\mathbb{E} \left[-2 \log A(p_{\widehat{\mathbf{M}}}(\mathbf{M}), p_{\mathbf{M}^*}(\mathbf{M})) \right]}{nm} &\leq \frac{8C_D \log s}{s} + 3 \min_{\mathbf{H} \in \mathcal{H}} \left\{ \frac{D(p_{\mathbf{M}^*}(\mathbf{M}) \| p_{\mathbf{H}}(\mathbf{M}))}{nm} + \left(\xi + \frac{4C_D \log 2}{3} \right) \right. \\ &\quad \left. d \log_2(K) \times \frac{(m+n+2)d^{-1} + |\mathcal{G}(\mathbf{X})| + |\mathcal{G}(\mathbf{Y})|}{s} \right\}. \end{aligned} \quad (59)$$

Let $\lambda = 2\sigma^2 \xi d \log_2(K)$. Recalling that $\xi \geq (1 + 2C_D/3) 2 \log 2$ and using the fact that $\log_2(K) = \lceil \mu \log_2(n_0) \rceil \leq 2\mu \log(n_0) / \log 2$, we have, for

$$\lambda \geq 8\sigma^2 \mu d (1 + 2C_D/3) \log(n_0), \quad (60)$$

the estimate

$$\widehat{\mathbf{M}}(\Omega, \Phi_{\Omega}(\mathbf{M})) = \arg \min_{\mathbf{H} \in \mathcal{H}} \left\{ -\log p_{\mathbf{H}}(\Phi_{\Omega}(\mathbf{M})) + \frac{\lambda}{2\sigma^2} (|\mathcal{G}(\mathbf{X})| + |\mathcal{G}(\mathbf{Y})|) \right\} \quad (61)$$

satisfies

$$\begin{aligned} \frac{\mathbb{E} \left[-2 \log A(p_{\widehat{\mathbf{M}}}(\mathbf{M}), p_{\mathbf{M}^*}(\mathbf{M})) \right]}{nm} &\leq \frac{8C_D \log s}{s} + 3 \min_{\mathbf{H} \in \mathcal{H}} \left\{ \frac{D(p_{\mathbf{M}^*}(\mathbf{M}) \| p_{\mathbf{H}}(\mathbf{M}))}{nm} \right. \\ &\quad \left. + \left(\frac{\lambda}{2\sigma^2} + \frac{8\mu d C_D \log(n_0)}{3} \right) \times \frac{(m+n+2)d^{-1} + |\mathcal{G}(\mathbf{X})| + |\mathcal{G}(\mathbf{Y})|}{s} \right\}. \end{aligned} \quad (62)$$

Recall that the noise matrix \mathbf{N} contains i.i.d. elements following $\mathcal{N}(0, \sigma^2)$ and the pdf of the observations $\Phi_{\Omega}(\mathbf{M})$ is

$$p_{\mathbf{H}}(\Phi_{\Omega}(\mathbf{M})) = \frac{1}{(2\pi\sigma^2)^{|\Omega|/2}} \exp \left(-\frac{\|\Phi_{\Omega}(\mathbf{M} - \mathbf{H})\|_F^2}{2\sigma^2} \right). \quad (63)$$

Combining (61) and (63), we have,

$$\widehat{\mathbf{M}}(\Omega, \Phi_{\Omega}(\mathbf{M})) = \arg \min_{\mathbf{H} \in \mathcal{H}} \left\{ \|\Phi_{\Omega}(\mathbf{M} - \mathbf{H})\|_F^2 + \lambda (|\mathcal{G}(\mathbf{X})| + |\mathcal{G}(\mathbf{Y})|) \right\}. \quad (64)$$

Furthermore, we have

$$\begin{aligned}
\mathbb{D}(p_{M_{ij}^*}(M_{ij})||p_{H_{ij}}(M_{ij})) &= \int_{-\infty}^{\infty} \frac{H_{ij}^2 - (M_{ij}^*)^2 + 2(M_{ij}^* - H_{ij})x}{2\sigma^2} p_{M_{ij}^*}(x) dx \\
&= \frac{1}{2\sigma^2} \left(H_{ij}^2 - (M_{ij}^*)^2 + 2(M_{ij}^* - H_{ij}) \int_{-\infty}^{\infty} x p_{M_{ij}^*}(x) dx \right) \\
&= 2\sigma^{-2} (H_{ij} - M_{ij}^*)^2,
\end{aligned} \tag{65}$$

where the last inequality follows from the fact that $\int_{-\infty}^{\infty} x p_{M_{ij}^*}(x) dx = M_{ij}^*$. Then, recalling (53) and noting that $\|\mathbf{H}\|_{\infty} \leq C_m$ for each $\mathbf{H} \in \mathcal{H}$, we choose $C_D = 2C_m^2/\sigma^2$ and thus (60) becomes

$$\lambda \geq 8\mu d \left(\sigma^2 + \frac{4C_m^2}{3} \right) \log(n_0). \tag{66}$$

Using a similar approach, we obtain

$$-\log A(p_{M_{ij}^*}(M_{ij}), p_{H_{ij}}(M_{ij})) = \frac{(H_{ij} - M_{ij}^*)^2}{8\sigma^2}. \tag{67}$$

Based on (65) and (67), the inequality (62) can be rewritten as

$$\begin{aligned}
\frac{\mathbb{E} \left[\|\widehat{\mathbf{M}} - \mathbf{M}^*\|_F^2 \right]}{nm} &\leq \frac{64C_m^2 \log s}{s} + 6 \min_{\mathbf{H} \in \mathcal{H}} \left\{ \frac{\|\mathbf{H} - \mathbf{M}^*\|_F^2}{nm} + \left(\lambda + \frac{32\mu d C_m^2 \log(n_0)}{3} \right) \times \right. \\
&\quad \left. \frac{(m+n+2)d^{-1} + |\mathcal{G}(\mathbf{X})| + |\mathcal{G}(\mathbf{Y})|}{s} \right\}.
\end{aligned} \tag{68}$$

Next, we prove an upper bound for $\min_{\mathbf{H} \in \mathcal{H}} \|\mathbf{H} - \mathbf{M}^*\|_F^2$. Let $\mathbf{H}_0 = \mathbf{X}_0 \mathbf{Y}_0^T \in \mathcal{M}$ be a candidate reconstruction such that the entries of \mathbf{X}_0 and \mathbf{Y}_0 are the closest discretized surrogates of the entries of \mathbf{X}^* and \mathbf{Y}^* , respectively. Recalling (17) and (16), we have, $\|\mathbf{X}_0 - \mathbf{X}^*\|_F^2 \leq 4dnC_x^2/K^2$ and $\|\mathbf{Y}_0 - \mathbf{Y}^*\|_F^2 \leq 4dmC_y^2/K^2$, which, in conjunction with $\mathbf{H}_0 = \mathbf{X}_0 \mathbf{Y}_0^T$, implies

$$\begin{aligned}
\|\mathbf{H}_0 - \mathbf{M}^*\|_F &= \|\mathbf{X}_0 \mathbf{Y}_0^T - \mathbf{X}^* (\mathbf{Y}^*)^T\|_F \leq \|\mathbf{X}_0 - \mathbf{X}^*\|_F \|\mathbf{Y}_0\|_F + \|\mathbf{X}^*\|_F \|\mathbf{Y}_0 - \mathbf{Y}^*\|_F \\
&\leq \frac{4dC_x C_y \sqrt{nm}}{K} \leq \frac{4dC_x C_y \sqrt{nm}}{\mu \log(n_0)}.
\end{aligned} \tag{69}$$

Using (69), we obtain

$$\|\mathbf{H}_0 - \mathbf{M}^*\|_F^2 / (nm) \leq 16dC_x^2 C_y^2 / (\mu \log(n_0))^2,$$

which, together with the fact that $|\mathcal{G}(\mathbf{X}_0)| + |\mathcal{G}(\mathbf{Y}_0)| = |\mathcal{G}(\mathbf{X}^*)| + |\mathcal{G}(\mathbf{Y}^*)|$, implies

$$\begin{aligned}
\frac{\mathbb{E} \left[\|\widehat{\mathbf{M}} - \mathbf{M}^*\|_F^2 \right]}{nm} &\leq \frac{64C_m^2 \log s}{s} + \frac{96dC_x^2 C_y^2}{(\mu \log(n_0))^2} + (6\lambda + 64\mu C_m^2 \log(n_0)) \times \\
&\quad \frac{(m+n+2) + (|\mathcal{G}(\mathbf{X}^*)| + |\mathcal{G}(\mathbf{Y}^*)|)d}{s}.
\end{aligned} \tag{70}$$

Letting $C_1 = 64C_m^2$, $C_2 = 96dC_x^2 C_y^2$, $C_3 = 64C_m^2$ and using (64), (66), (70), we finish the proof.

G Parameter Tuning on γ_X and γ_Y

In this section, we introduce an efficient way to improve the final results. Notably this process also generates a solution path with a hierarchical structure of the subgroups. Suppose we aim to find the optimal $(\gamma_X, \gamma_Y) \in [a_x, b_x] \times [a_y, b_y]$ using, e.g., cross-validation. Let (γ_X^u, γ_Y^v) , $u, v \in N$ be a grid of values such that $a_x = \gamma_X^1 < \gamma_X^2 < \dots < \gamma_X^{N_x} = b_x$ and $a_y = \gamma_Y^1 < \gamma_Y^2 < \dots < \gamma_Y^{N_y} = b_y$, where $\gamma_X^{u+1} - \gamma_X^u = h$ and $\gamma_Y^{v+1} - \gamma_Y^v = h$ for a small $h > 0$. Following the sequence $(n = u + v, u \leq v, n = 2, 3, \dots)$, we define the next value of (u, v) be to (u^+, v^+) on a zig-zag path. The tuning process always uses the solution of the optimization problem (3) with (γ_X^u, γ_Y^v) as the initial values for the next round of optimization with $(\gamma_X^{u^+}, \gamma_Y^{v^+})$.

H More Experimental Results

H.1 More Results on Synthetic Data

To show the performance improvement, we examine the average relative error w.r.t the sample rate and σ . In this simulation, we set $n = 100$, $k_x = k_y = 40$ and $\gamma_X = \gamma_Y = 10$. For each fixed pair of values for the sample rate and σ , we compute the average relative error by averaging over 50 Monte Carlo trials. Fig. 8 shows that the blue region with smaller relative error becomes much larger when using the pairwise fusion.

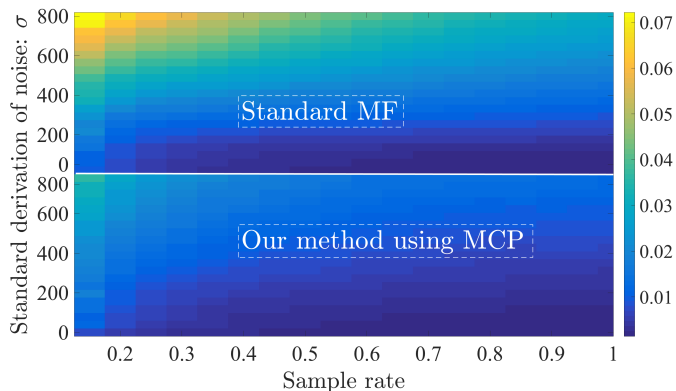


Figure 8: Average relative error w.r.t. sample rate and σ : the standard MF (up) and our method (down).

H.2 Running Time Comparison

In this section, we demonstrate that our proposed CG based solver (13) can significantly speed up the algorithm. We test the performance using the synthetic data in Section 5.3, where we set $n = 200$, $k_x = k_y = 200$, $\delta = 100$ and the sample rate $\rho = 0.12$. We choose $n = 200$ for a comparison because the exact solver fails for $n \geq 500$. Fig. 9 shows that our approach is almost 2 orders of magnitude faster than the one that solve the equation (12) exactly.

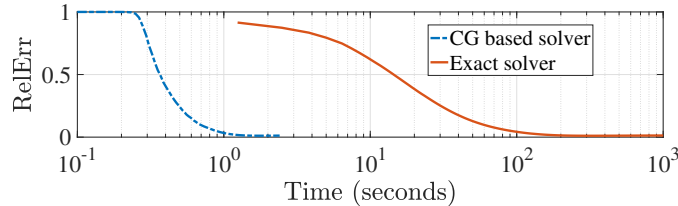


Figure 9: Relative error $\|\widehat{\mathbf{M}} - \mathbf{M}\|_F / \|\mathbf{M}\|_F$ against the running time.

H.3 MovieLens and Jester Data Statistics

The statistics of collaborate filtering datasets used in our experiments is presented in Table 5.

Table 5: Data statistics

Datasets	# of users (n)	# of items (m)	Density
Jester1	24983	100	0.7247
Jester2	23500	100	0.7272
Jester3	24938	100	0.2474
MovieLens100K	943	1682	0.0630
MovieLens1M	6040	3706	0.0447

H.4 Matrix Completion on Images

We compare our algorithm to four state-of-the-art matrix completion algorithms: nonnegative matrix factorization completion (NMFC) (Xu et al., 2012), singular vector thresholding (SVT) (Cai et al., 2010), fixed point continuation with approximate SVD (FPCA) (Ma et al., 2011b) and low rank matrix fitting (LMaFit) (Wen et al., 2012) on image recovery. The matlab codes of these methods are downloaded from the authors’ websites. Our test data consist of four grayscale images, including 752×500 “Flower”, 360×360 “Dresser”, 512×512 “Lena”, and 503×880 “Diver”.

We randomly sample $w\% \in \{5\%, 10\%, 20\%\}$ of the pixels from the original image for training, and randomly sample 10% of the remaining pixels for validation. Using 4-fold cross validation on training data, we select d from $\{5, 10, 15\}$, $\eta = 2.25 \times 10^3$ and $\alpha = 0.02$. In addition, we adopt the first way described in (22) to compute w_{ij} and u_{st} , with $k_w = k_u$ selected from $\{5, 10\}$. The parameters for FPCA, SVT, NMFC and LMaFit have been optimized for a fair comparison. We evaluate the recovery qualities using the relative error

$$\text{RelErr} = \|\widehat{\mathbf{M}} - \mathbf{M}\|_F / \|\mathbf{M}\|_F,$$

where $\widehat{\mathbf{M}}$ is the reconstructed solution based on the optimization and \mathbf{M} is the original matrix. The experimental results are given in Table 6, where the running time of LMaFit written in C++ is not listed. It can be seen from Table 6 that our method achieves an average of more than 20% improvement for the relative error and is comparable in running time with FPCA and SVT.

Table 6: Image recovery: the relative error is computed using the average over 10 trials

Image	Algorithm	time RelErr		time RelErr		time RelErr	
		$w\%=5\%$		$w\%=10\%$		$w\%=20\%$	
Flower	LLFMC (Lasso)	1.42×10^1	3.63×10^{-1}	1.64×10^1	2.79×10^{-1}	2.49×10^1	2.00×10^{-1}
	SVT	1.19×10^2	8.73×10^{-1}	1.54×10^2	7.79×10^{-1}	1.61×10^2	6.98×10^{-1}
	NMFC	1.21×10^1	4.92×10^{-1}	1.43×10^1	3.96×10^{-1}	2.21×10^1	3.03×10^{-1}
	FPCA	1.25×10^2	4.31×10^{-1}	1.73×10^2	4.12×10^{-1}	2.02×10^2	2.91×10^{-1}
	LMaFit	—	4.75×10^{-1}	—	3.65×10^{-1}	—	2.86×10^{-1}
Dresser	LLFMC (Lasso)	1.35×10^1	7.18×10^{-2}	1.41×10^1	5.04×10^{-2}	2.43×10^1	3.76×10^{-2}
	SVT	1.55×10^1	9.25×10^{-1}	3.19×10^1	8.14×10^{-1}	7.13×10^1	7.62×10^{-1}
	NMFC	1.33×10^1	8.98×10^{-2}	1.32×10^1	6.56×10^{-2}	1.16×10^1	4.64×10^{-2}
	FPCA	3.77×10^1	9.82×10^{-2}	3.19×10^1	8.46×10^{-2}	7.13×10^1	6.58×10^{-2}
	LMaFit	—	8.99×10^{-2}	—	8.30×10^{-2}	—	5.97×10^{-2}
Lena	LLFMC (Lasso)	3.10×10^1	2.45×10^{-1}	4.93×10^1	1.75×10^{-1}	5.04×10^1	1.23×10^{-1}
	SVT	1.17×10^2	8.94×10^{-1}	1.26×10^2	8.65×10^{-1}	1.96×10^2	6.81×10^{-1}
	NMFC	1.67×10^1	2.89×10^{-1}	1.68×10^1	2.06×10^{-1}	1.85×10^1	1.36×10^{-1}
	FPCA	1.20×10^2	2.95×10^{-1}	1.40×10^2	2.01×10^{-1}	1.96×10^2	1.46×10^{-1}
	LMaFit	—	2.92×10^{-1}	—	2.10×10^{-1}	—	1.49×10^{-1}
Diver	LLFMC (Lasso)	1.69×10^1	1.86×10^{-1}	1.78×10^1	1.38×10^{-1}	1.82×10^1	1.13×10^{-1}
	SVT	1.21×10^2	8.81×10^{-1}	1.12×10^2	8.01×10^{-1}	8.01×10^1	6.91×10^{-1}
	NMFC	2.11×10^1	2.18×10^{-1}	2.06×10^1	1.66×10^{-1}	2.13×10^1	1.33×10^{-1}
	FPCA	1.86×10^2	2.15×10^{-1}	1.83×10^2	1.72×10^{-1}	2.60×10^2	1.37×10^{-1}
	LMaFit	—	2.16×10^{-1}	—	1.78×10^{-1}	—	1.37×10^{-1}

References

- Bapat, Ravindra B. *Graphs and matrices*, volume 27. Springer, 2010.
- Bennett, James, Lanning, Stan, and Netflix, Netflix. The netflix prize. In *In KDD Cup and Workshop in conjunction with KDD*, 2007.
- Boyd, Stephen, Parikh, Neal, Chu, Eric, Peleato, Borja, and Eckstein, Jonathan. Distributed optimization and statistical learning via the alternating direction method of multipliers. *Found. Trends Mach. Learn.*, 3(1): 1–122, January 2011.
- Cai, Jian-Feng, Candès, Emmanuel J, and Shen, Zuowei. A singular value thresholding algorithm for matrix completion. *SIAM Journal on Optimization*, 20(4):1956–1982, 2010.
- Candès, Emmanuel J and Recht, Benjamin. Exact matrix completion via convex optimization. *Foundations of Computational Mathematics*, 9(6):717, 2009.
- Chiang, Kai-Yang, Hsieh, Cho-Jui, and Dhillon, Inderjit S. Matrix completion with noisy side information. In *Advances in Neural Information Processing Systems*, pp. 3447–3455, 2015.
- Cover, Thomas M and Thomas, Joy A. *Elements of information theory*. John Wiley & Sons, 2012.
- Deng, Wei, Lai, Ming-Jun, Peng, Zhimin, and Yin, Wotao. Parallel multi-block ADMM with $o(1/k)$ convergence. *Journal of Scientific Computing*, 71(2):712–736, 2017.

- Fan, Jianqing and Li, Runze. Variable selection via nonconcave penalized likelihood and its oracle properties. *Journal of the American Statistical Association*, 96(456):1348–1360, 2001.
- Goldberg, Ken, Roeder, Theresa, Gupta, Dhruv, and Perkins, Chris. Eigentaste: A constant time collaborative filtering algorithm. *information retrieval*, 4(2):133–151, 2001.
- Gopalan, Prem K, Charlin, Laurent, and Blei, David. Content-based recommendations with poisson factorization. In *Advances in Neural Information Processing Systems*, pp. 3176–3184, 2014.
- Han, Lei and Zhang, Yu. Learning multi-level task groups in multi-task learning. In *AAAI*, pp. 2638–2644, 2015.
- Harper, F Maxwell and Konstan, Joseph A. The movielens datasets: History and context. *ACM Transactions on Interactive Intelligent Systems (TiiS)*, 5(4):19, 2016.
- He, Bingsheng, Hou, Liusheng, and Yuan, Xiaoming. On full jacobian decomposition of the augmented lagrangian method for separable convex programming. *SIAM Journal on Optimization*, 25(4):2274–2312, 2015.
- Hong, Mingyi, Luo, Zhi-Quan, and Razaviyayn, Meisam. Convergence analysis of alternating direction method of multipliers for a family of nonconvex problems. *SIAM Journal on Optimization*, 26(1):337–364, 2016.
- Jiacheng, Xu. Family shopping recommendation system using user profile and behavior data. *arXiv preprint arXiv:1708.07289*, 2017.
- Kalofolias, Vassilis, Bresson, Xavier, Bronstein, Michael, and Vandergheynst, Pierre. Matrix completion on graphs. *arXiv preprint arXiv:1408.1717*, 2014.
- Kim, Jingu, Monteiro, Renato DC, and Park, Haesun. Group sparsity in nonnegative matrix factorization. In *Proceedings of the 2012 SIAM International Conference on Data Mining*, pp. 851–862. SIAM, 2012.
- Koltchinskii, Vladimir, Lounici, Karim, Tsybakov, Alexandre B, et al. Nuclear-norm penalization and optimal rates for noisy low-rank matrix completion. *The Annals of Statistics*, 39(5):2302–2329, 2011.
- Koren, Yehuda, Bell, Robert, and Volinsky, Chris. Matrix factorization techniques for recommender systems. *Computer*, 42(8):30–37, August 2009. ISSN 0018-9162.
- Li, Guoyin and Pong, Ting Kei. Global convergence of splitting methods for nonconvex composite optimization. *SIAM Journal on Optimization*, 25(4):2434–2460, 2015.
- Ma, Hao, Zhou, Dengyong, Liu, Chao, Lyu, Michael R, and King, Irwin. Recommender systems with social regularization. In *Proceedings of the fourth ACM international conference on Web search and data mining*, pp. 287–296. ACM, 2011a.
- Ma, Shiqian, Goldfarb, Donald, and Chen, Lifeng. Fixed point and bregman iterative methods for matrix rank minimization. *Mathematical Programming*, 128(1-2):321–353, 2011b.
- Ma, Shujie and Huang, Jian. A concave pairwise fusion approach to subgroup analysis. *Journal of the American Statistical Association*, 112(517):410–423, 2017.

- Monti, Federico, Bronstein, Michael, and Bresson, Xavier. Geometric matrix completion with recurrent multi-graph neural networks. In *Advances in Neural Information Processing Systems*, pp. 3700–3710, 2017.
- Rao, Nikhil, Yu, Hsiang-Fu, Ravikumar, Pradeep K, and Dhillon, Inderjit S. Collaborative filtering with graph information: Consistency and scalable methods. In *Advances in Neural Information Processing Systems*, pp. 2107–2115, 2015.
- Soni, Akshay, Jain, Swayambhoo, Haupt, Jarvis, and Gonella, Stefano. Noisy matrix completion under sparse factor models. *arXiv preprint arXiv:1411.0282*, 2014.
- Wang, Fenghui, Cao, Wenfei, and Xu, Zongben. Convergence of multi-block bregman ADMM for nonconvex composite problems. *arXiv preprint arXiv:1505.03063*, 2015a.
- Wang, Huahua and Banerjee, Arindam. Bregman alternating direction method of multipliers. In *Advances in Neural Information Processing Systems*, pp. 2816–2824, 2014.
- Wang, Yu, Yin, Wotao, and Zeng, Jinshan. Global convergence of admm in nonconvex nonsmooth optimization. *arXiv preprint arXiv:1511.06324*, 2015b.
- Wen, Zaiwen, Yin, Wotao, and Zhang, Yin. Solving a low-rank factorization model for matrix completion by a nonlinear successive over-relaxation algorithm. *Mathematical Programming Computation*, 4(4):333–361, 2012.
- Xu, Yangyang, Yin, Wotao, Wen, Zaiwen, and Zhang, Yin. An alternating direction algorithm for matrix completion with nonnegative factors. *Frontiers of Mathematics in China*, 7(2):365–384, 2012.
- Zhang, Cun-Hui. Nearly unbiased variable selection under minimax concave penalty. *The Annals of Statistics*, 38(2):894–942, 2010.
- Zhao, Zhou, Zhang, Lijun, He, Xiaofei, and Ng, Wilfred. Expert finding for question answering via graph regularized matrix completion. *IEEE Transactions on Knowledge and Data Engineering*, 27(4):993–1004, 2015.
- Zou, Hui. The adaptive lasso and its oracle properties. *Journal of the American Statistical Association*, 101(476):1418–1429, 2006.